E R R A T U M

Photograph for Figure 17a, page 27, became inverted in printing process.

ST. ANTHONY FALLS HYDRAULIC LABORATORY
UNIVERSITY OF MINNESOTA

Project Report No. 46

EXPERIMENTAL STUDIES OF PNEUMATIC AND HYDRAULIC BREAKWATERS

Submitted by
LORENZ G. STRAUB
Director

Prepared by
J. M. WETZEL

May, 1955

Prepared for the
OFFICE OF NAVAL RESEARCH
Department of the Navy
Washington, D.C.

Office of Naval Research Project No. NR 062-178, Contract Nonr-710(10)

P R E F A C E

Several types of portable breakwaters are available to reduce the destructive action of waves. Two of these types--the pneumatic and hydraulic breakwaters--reduce wave energy by creating a surface current that opposes the direction of wave propagation. Several prototype installations have been made utilizing the pneumatic breakwater, and they have met with various degrees of success. It is not known if hydraulic breakwaters have been employed on a large scale, as published data or descriptions of such a breakwater have not been found. Limited small-scale laboratory studies were made of both breakwaters, but little information is available describing these tests. To create a better understanding of the parameters involved in wave absorption by the pneumatic and hydraulic breakwaters, it appears necessary to conduct further laboratory studies utilizing both systems.

The small-scale studies described in this report are pilot studies for tests to be conducted in a 9-ft wave tank. The experimental studies were conducted to secure basic information concerning the pertinent parameters, and as the studies are of a preliminary nature, the results should not be considered as refined design data.

The studies covered in this report were carried out during the period April 1, 1954 to December 1, 1954. The project was sponsored by the Office of Naval Research under Project NR 062-178, Contract Nonr 710(10).

The entire program was under the general direction of Dr. Lorenz G. Straub, director of the Laboratory. C. E. Bowers, as project leader, critically reviewed this report and was responsible for the supervision and progress of the project as a whole. The study was conducted and the report written by J. M. Wetzel. The experimental work was performed mainly by Gerald Nelson.

Preparation of the manuscript for printing was carried out by Maxine Chapin under the general supervision of Professor Loyal Johnson.

A B S T R A C T

Pilot studies of pneumatic, and vertical and horizontal hydraulic breakwaters were conducted in a small glass-walled wave channel to determine the effect of various parameters on wave attenuation. The data are preliminary and are to be checked in a large wave tank.

A theory of the pneumatic breakwater by G. I. Taylor is briefly summarized, and part of this theory is verified by experimental data. In the experimental studies, emphasis was placed on tests of the vertical and horizontal water-jet breakwaters. The parameters considered were wave length, wave steepness, water depth, jet discharge, jet velocity, and jet submergence. In general, wave steepness was of minor importance. Both the pneumatic and hydraulic breakwaters proved to be effective in attenuating deep-water waves, but neither were effective for shallow-water waves. The power requirements of the vertical water jets for a specific wave length to water depth ratio (L/d) and attenuation were considerably higher than the horizontal water jets; the pneumatic breakwater required less power than the horizontal water jets in the larger L/d region.

C O N T E N T S

LIST OF ILLUSTRATIONS

Figure		Page

LIST OF SYMBOLS

a_1 - Wave amplitude at upper surface of current.

a_2 - Wave amplitude at lower surface of current.

c - Specific heat of air.

d - Water depth.

e - Base of natural logarithms.

f - Horizontal jet submergence.

g - Acceleration of gravity.

h - Surface current depth.

h_o - Initial surface current depth.

i - $\sqrt{-1}$.

m - $2\pi/L$.

t - Time.

v_x - Vertical velocity at distance x from center of current.

w - Unit weight of water.

x - Horizontal distance from origin of current.

y - Vertical distance above still-water surface.

B_1 - Arbitrary constant.

B_2 - Arbitrary constant.

C - Wave celerity.

C_1 - Arbitrary constant.

C_g - Group velocity.

E - Total energy of wave.

H - Wave height.

H_I - Incident wave height.

H_R - Reflected wave height.

H_T - Transmitted wave height.

L - Wave length.

Q_A - Air discharge.

Q_H - Total discharge of heat.

Q_W - Water discharge.

T - Wave period; also temperature.

T_p - Period of pulsating jets.

U_k - Uniform current velocity.

U_{k_o} - Initial uniform or mean current velocity.

U_o - Initial maximum surface current velocity; also maximum velocity at center of vertical current.

U_x - Maximum surface velocity at distance x.

V_j - Jet velocity.

γ - Dimensionless parameter.

ζ - Temperature difference between heated air and atmosphere.

κ - Proportion of bubbles in any volume.

ξ - Dimensionless parameter.

π - 3.1416.

ρ_a - Density of air.

σ - $2\pi/T$.

ω - Dimensionless parameter.

ϕ_1 - Velocity potential.

ϕ_2 - Velocity potential.

EXPERIMENTAL STUDIES OF PNEUMATIC AND HYDRAULIC BREAKWATERS

I. INTRODUCTION

The concept of using a portable device for reducing the destructive action of waves is not a recent innovation. As early as 1907, Philip Brasher [1]* patented a method of subduing waves by forcing compressed air through a submerged perforated pipe. His notion that the vertical force produced by the air bubbles would "take the feet out from under the waves" was not necessarily correct, yet his pneumatic breakwater met with some success. Prototype installations in 1908 at Million Dollar Pier, Atlantic City, and in 1915 at El Segundo Pier, California, were successful in damping waves. However, other installations tested about 1937 were not successful, and many other reports of the system are conflicting and controversial. In all cases, very little useful information has been given describing the tests.

Several small-scale studies have been made by early experimenters in England and Russia, but few data have been made available. The small-scale studies described in this report were conducted to provide information on the parameters affecting the damping of waves, utilizing air and water jets. The data presented herein are the results of tests conducted in a 6-in. width glass-walled channel and are to be considered preliminary. A separate report describing the tests in a 9-ft wave tank will be presented upon completion of the large-scale tests.

II. GENERAL CONSIDERATIONS

A pneumatic breakwater is a bubble screen formed by passing compressed air through a submerged, perforated pipe. While rising to the surface the air bubbles induce a vertical current. The vertical current produces a circulation of the water, with horizontal currents away from the screen near the free surface and toward the screen near the lower boundary. Two symmetrical branches of the horizontal surface current are formed, one moving upstream of the breakwater and the other downstream. The surface horizontal

*Numbers in brackets refer to the Bibliography on p. 45.

currents diminish as they progress away from the screen. It has been found that the surface current moving against the direction of wave propagation is largely responsible for attenuation, the other branch contributing little toward absorbing the wave. The breakwater is effective in attenuating deep-water waves but has little effect on shallow-water waves.

The hydraulic or water-jet breakwater is very similar, being formed by forcing water through a perforated pipe. This type of breakwater can be utilized in two positions with the jets directed either vertical or horizontal. In either position a surface current will be induced by the water jets. This current, as will be seen later, is very similar in profile to that induced by the air bubbles. With the vertical jet system, the distribution pipe is located at the bed of the channel, with the water jets directed upward, inducing an upward current in the surrounding liquid. As this current approaches the surface it spreads out symmetrically into two branches parallel to the surface. The circulation pattern is similar to the pattern of the pneumatic breakwater.

The horizontal jets are submerged slightly below the water surface, and are directed to oppose the direction of wave propagation. In this case the downstream surface current is not developed, and most of the jet energy is available for creating a more effective surface current.

Utilizing either type jet, the high velocity portion of the induced current is confined to a region near the surface. With such currents, the best results could be expected for deep-water waves with the effectiveness decreasing rapidly for the shallow-water waves. The experimental data in Section V verifies this statement.

There has been limited information published on portable breakwaters of the jet type. Most of the available information concerns the pneumatic breakwater, but little discussion is given to test results that can be used as a comparison basis for the current studies. A British report [2] that summarizes some of the previous experiments provides data on model and prototype scales, although these data are incomplete. Several small-scale tests were made in England and Russia on the pneumatic breakwater in the 1930's, where it was found that the bubble barrier was ineffective for long waves in shallow water but did have considerable effect on the shorter waves. At Teddington, England, tank experiments were conducted on the Brasher air breakwater, but they did not prove a success, and no test data have been published. Mention is made that water jets were tried but again no results were published.

Other small-scale tests of the pneumatic breakwater were performed by Schijf [3]. His primary interest was to determine air quantities necessary to absorb waves of given characteristics. His results indicated that the required air discharge was largely dependent on wave length for a given depth of water, wave height or steepness being of minor importance. However, considerable difficulty was encountered in attempting to extrapolate the model data to prototype conditions. The computed requirements were much in excess of the requirements of an actual prototype installation. Sufficient data were not available to determine the existence of scale effect.

Perhaps the most significant work in the United States has been done by Carr [4]. He has investigated both the pneumatic and hydraulic breakwaters, but unfortunately the published data on his tests are limited. It appears that his primary concern was in examining the breakwater for a possible use in damping large storm waves. On this basis his conclusions were similar to those from other experiments previously made: that neither type of breakwater was effective for long waves in shallow water. Carr also studied a form of horizontal jet breakwater that created a uniform current the entire depth of channel, and found it was effective for stopping shallow-water waves. However, the power requirements of the system were high.

III. THEORETICAL CONSIDERATIONS

There has been little theoretical work published as to the reason the pneumatic breakwater is effective in attenuating deep-water waves. Shortly after Brasher devised the system, several theories were suggested but were later proved to be of no value. G. I. Taylor [5] proposed the most useful theory on stopping waves by means of a curtain of bubbles. He suggested that the damping of waves is caused by the horizontal current which spreads out from the region where the vertical current induced by the rising bubbles reaches the surface. The analysis considered the effect of the surface current on the transmission of deep-water waves, and a brief summary of the analysis is given here. Taylor also suggested that the bubbles themselves do not dampen the waves any appreciable amount, as the change in density in the bubble region is very small.

Consider a current of depth h with a velocity U_k flowing over deep water. The reference axis is taken with x in the still-water surface and y measured upward, the lower surface of the current then being at $y = - h$. The velocity potential of the wave motion in the current region is

$$\phi_1 = - U_k x + \left(B_1 e^{my} + B_2 e^{-my}\right) e^{i(mx - \sigma t)} \tag{1}$$

and in the underlying water

$$\phi_2 = C_1 e^{m(y + h)} e^{i(mx - \sigma t)} \tag{2}$$

where

$$\frac{2\pi}{m} = L \text{ (wave length)}$$

$$\frac{2\pi}{\sigma} = T \text{ (wave period)}$$

The equations of the upper and lower surface of the current are, respectively,

$$y = a_1 e^{i(mx - \sigma t)} \tag{3}$$

$$y = - h + a_2 e^{i(mx - \sigma t)} \tag{4}$$

Combining the above equations with the continuity and pressure conditions at the surface and still-water interface, the resulting equation is

$$\left[(\sigma - mU_k)^4 - mg\sigma^2\right] \sinh mh + (\sigma - mU_k)^2 (\sigma^2 - mg) \cosh mh = 0 \tag{5}$$

To find a solution that is useful in discussing the modification of waves in the current region, it is necessary to find the roots of Eq. (5) with a given σ, with m regarded as the variable. In other words, the wave period remains constant as the same number of waves pass a given point in a given time, but the wave length and celerity will change.

As Eq. (5) is transcendental, it is difficult to present a complete discussion of its roots. By numerical methods, the real roots can be investigated, and the changes in velocity or wave length corresponding with any given values of surface current and current depth can be determined.

Letting $\gamma = \dfrac{mU_k}{\sigma}$, $\xi = \dfrac{g}{U_k \sigma}$, $\omega = \dfrac{hg}{U_k^{\,2}}$

Equation (5) is written in the form

$$\frac{(1-\gamma)^2\,(1-\xi\gamma)}{(1-\gamma)^4-\xi\gamma} = -\tanh\left(\frac{\omega\gamma}{\xi}\right) \tag{6}$$

which can be solved numerically as shown in Fig. 1.

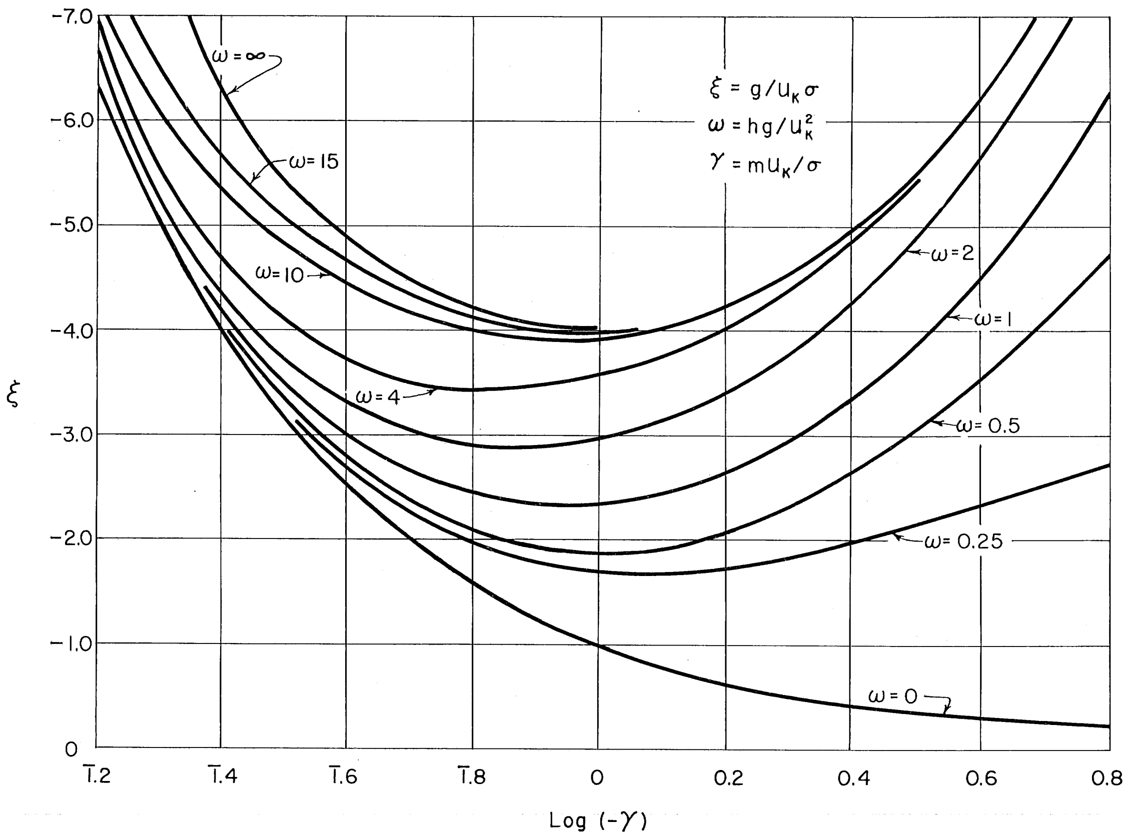

Fig. 1 - Numerical Solution of Taylor's Theory (Eq. 6)

The result of this numerical analysis represents all possible real solutions when the waves are opposing the direction of the current. It is seen that a minimum value of ξ occurs for each value of ω, and since $\sigma = g/U_k\xi$, the wave frequency has a maximum value. This maximum frequency corresponds to a specified wave length, for by definition

$$L = \frac{gT^2}{2\pi} = \frac{2\pi g}{\sigma^2} = 2\pi g \left(\frac{\xi U_k}{g}\right)^2 = \frac{2\pi U_k^{\,2}}{g} (\xi_{min})^2 \qquad (7)$$

where ξ_{min} is the minimum value of ξ for any given value of ω, or U_k and h, since $\omega = hg/U_k^{\,2}$.

To find the values of U_k and h to stop a given deep-water wave of length L, solve Eq. (7) for $U_k\,\xi_{min}$. By assuming any values of ω, ξ_{min} can be found from Fig. 1, thus determining values of U_k. Knowing U_k and the assumed value of ω, the current depth h can be found. The results are values of surface current and current depth necessary to stop all waves of lengths shorter than L. A typical computation is presented in Table I for $L = 50$ ft:

TABLE I

ω	ξ_{min}	U_k - ft/sec	h - ft
0.25	1.70	9.4	0.7
0.50	1.90	8.4	1.1
1.00	2.35	6.8	1.4
2.00	2.87	5.6	2.0
4.00	3.40	4.7	2.8
10.00	3.80	4.2	5.5
15.00	4.00	4.0	7.5

Any of the above values of U_k and h will stop waves of length less than 50 ft. However, Taylor suggested that this current must be maintained at least a wave length from the absorber. He proposed the following equation for spreading of the current

$$U_x^{\,2}(x + 5h_o) = 11.6\, h_o U_{k_o}^{\;2} \tag{8}$$

where U_x = maximum surface velocity at distance x, x = horizontal distance from origin of current, h_o = initial depth of current, and U_{k_o} = initial uniform or mean velocity.

Thus a current of velocity 6.8 fps and depth 1.4 ft will be reduced by mixing in 50 ft to 3.6 fps.

Taylor also indicated that a jet will spread in such a way that $hU_x^{\,2}$ is constant along the jet. Applying this principle to the above solution, the depth of the current will have increased to 5.0 ft. Since 3.6 fps is a maximum velocity, the mean velocity is about 1.8 fps at a depth of 5.0 ft, and from Table I, this is probably not sufficient to stop a 50-ft wave.

Another theoretical analysis by Taylor related the air discharge to currents induced by a curtain of bubbles by an analogy to the air currents above a horizontal line source of heat. Taylor extended some work by W. Schmidt and arrived at the result

$$U_o = 1.90 \left(\frac{Q_H g}{\rho_a c T} \right)^{1/3} \tag{9}$$

where ρ_a = density of air, c = specific heat of air, T = mean temperature, Q_H = total discharge of heat, and U_o = maximum velocity at center of vertical current.

The buoyancy caused by the bubbles is $1 - \kappa$ where κ is the proportion of bubbles in any volume. In the case of the heated-air column, the upward force is $T/(\zeta + T)$ where ζ is the temperature difference between the heated air and the atmosphere. Neglecting the expansion of the bubbles as they rise, the velocities of the bubbles in water and the heated-air currents are equal if $\kappa = \zeta/T$, assuming κ is small compared to 1, or ζ is small compared with T.

The total discharge of heat is

$$Q_H = \int \rho_a c v_x \zeta \, dx \tag{10}$$

where v_x = vertical velocity at distance x from center of current.

The total volume of bubbles crossing any section is

$$Q_A = \int \kappa v_x dx \tag{11}$$

The vertical currents in the two cases are equal if

$$Q_A = \frac{Q_H}{\rho_a c T} \tag{12}$$

Therefore:

$$U_o = 1.9 \, (Q_A g)^{1/3} \tag{13}$$

Expressing this equation in the English system

$$Q_A = 0.00454 \, U_o^3 \tag{14}$$

where Q_A = volume of air discharged, cfs/ft of pipe and U_o = maximum vertical current above the source.

As the vertical current approaches the surface, a horizontal current will spread out on each side with a maximum surface velocity of U_o. These currents will decrease in intensity and increase with depth as the distance from the source increases (Fig. 2). The streamlines shown in Fig. 2 are presented to illustrate the general circulation pattern.

Equation (14) also indicates that the maximum induced velocity is independent of air-release depth. The surface velocities remain the same for equal discharges, but the effective depth of the current changes in proportion to the depth of air release. For example, the velocity profile above the source extends to approximately 0.3 of the total depth of submergence. If the depth of submergence is increased, the velocity profile will also extend

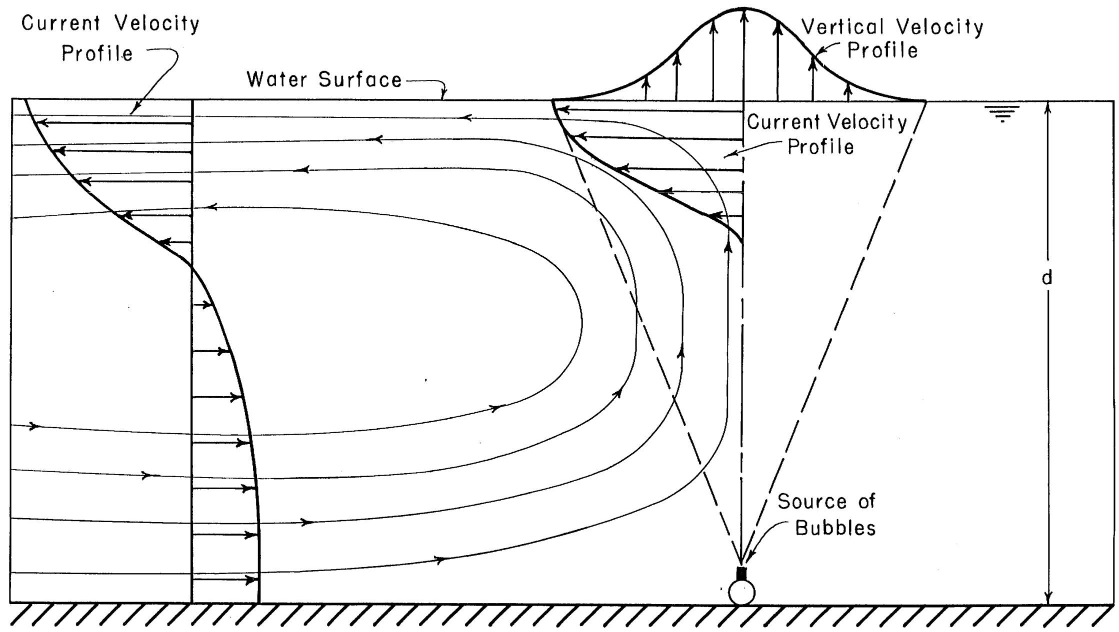

Fig. 2 - Qualitative Pattern of Surface Currents Produced by Air Bubbles [5]

to a greater depth, thereby creating a more effective current with less gradient. However, the horsepower requirements increase with water depth, thus dictating an optimum position of air release for a given L/d.

As the effective portion of the surface current is near the surface, one would expect that the current would have little effect on shallow-water waves, regardless of the strength of the current. From Eq. (14) an eightfold increase in discharge is necessary to double the maximum surface current. Thus, as the wave length increases in a given water depth, a point will be reached where any further increase in discharge will result in little change in the damping of the wave. This has been experimentally verified in the tests described in Section V.

Taylor's development assumed a uniform current distribution which does not completely represent the actual conditions. Of interest in connection with this problem is a theory presented by Biésel [6] concerning the propagation of waves in running water with a non-uniform velocity distribution. It was investigated to determine its applicability in this case. However, the equations became very complicated, and it was felt that the time required to solve the mathematical complexities could be used to better advantage in other phases of the study.

IV. EXPERIMENTAL STUDIES

A. Type of Studies

The experimental work on jet breakwaters consisted mainly of studies of the effect of various parameters on wave attenuation, defined as $1 - H_T/H_I$ where H_T/H_I is the ratio of transmitted to incident-wave height. Four jet types were utilized: (1) vertical air jets, (2) vertical water jets, (3) steady horizontal water jets, and (4) pulsating horizontal water jets. A definition sketch is shown in Fig. 3 for all types studied, the pulsating-jet arrangement being the same as that for the horizontal jets. With each jet type, the wave and jet characteristics were changed to determine their effect on attenuation. The parameters considered were: (1) wave length, (2) wave steepness, (3) jet diameter, (4) jet submergence, and (5) jet discharge. Not all of the above variables were studied with each jet type. The most extensive work has been done with the water jets upon request of the sponsor.

Some measurements were made of reflections caused by the jets and were found to be about 5 to 10 per cent, based on wave height. (The reflection coefficient is defined as H_R/H_I where H_R is the reflected wave height.)

With each of the jet types except the pulsating jets, the surface currents induced by the jets were measured in an attempt to relate the surface currents to available theory.

B. Test Facilities and Procedure

The small-scale tests of the pneumatic and hydraulic breakwaters were conducted in a glass-walled channel 6 in. wide, 16 in. deep, and 40 ft long (Fig. 4). A pendulum-type wave generator was used. At the opposite end of the channel an absorber was built with an absorption coefficient of about 95 per cent, based on wave height. (The absorption coefficient is defined as $1 - H_R/H_I$.) The breakwaters were located 17 ft downstream from the wave generator.

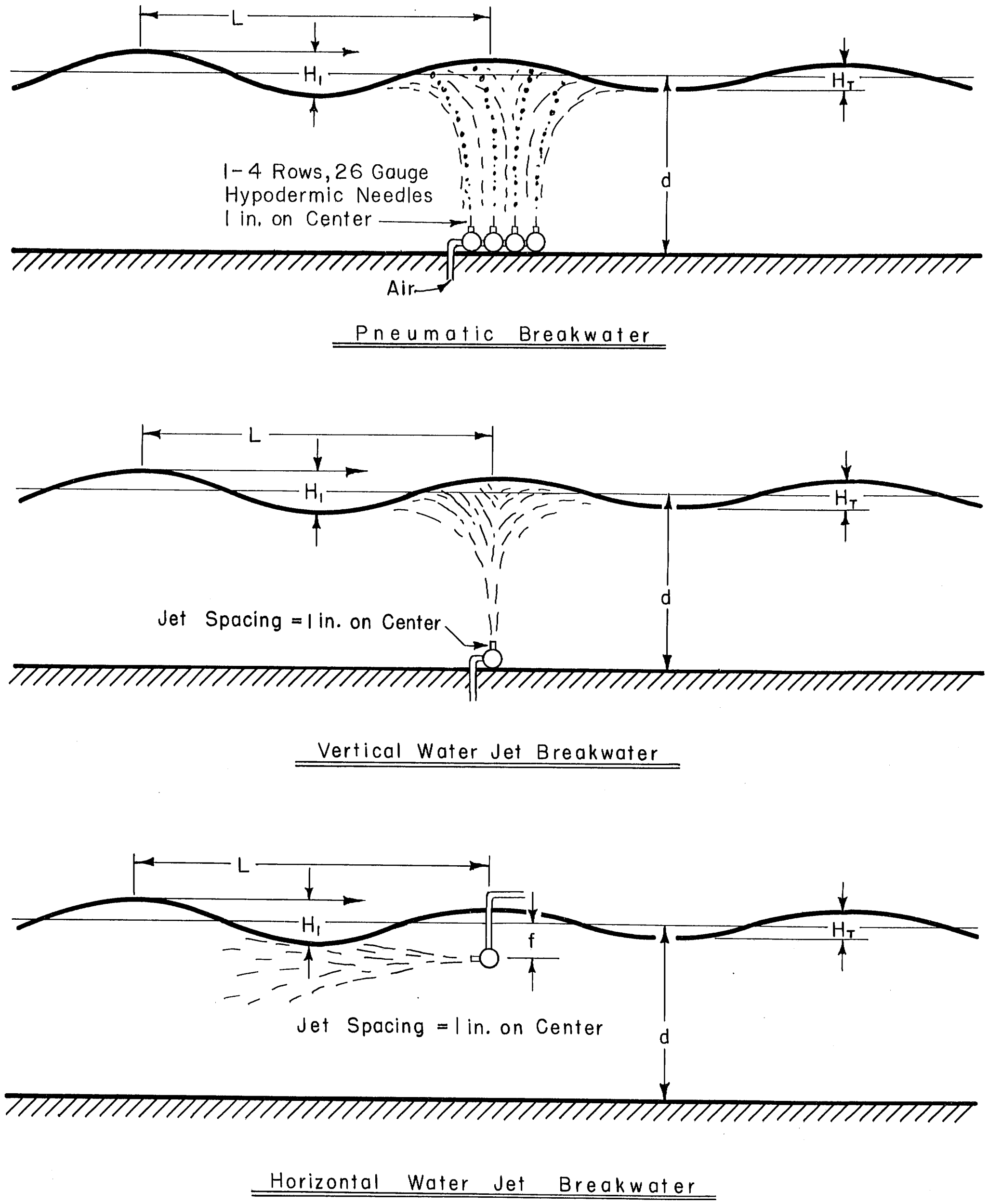

Fig. 3 – Definition Sketch of Pneumatic and Hydraulic Breakwaters

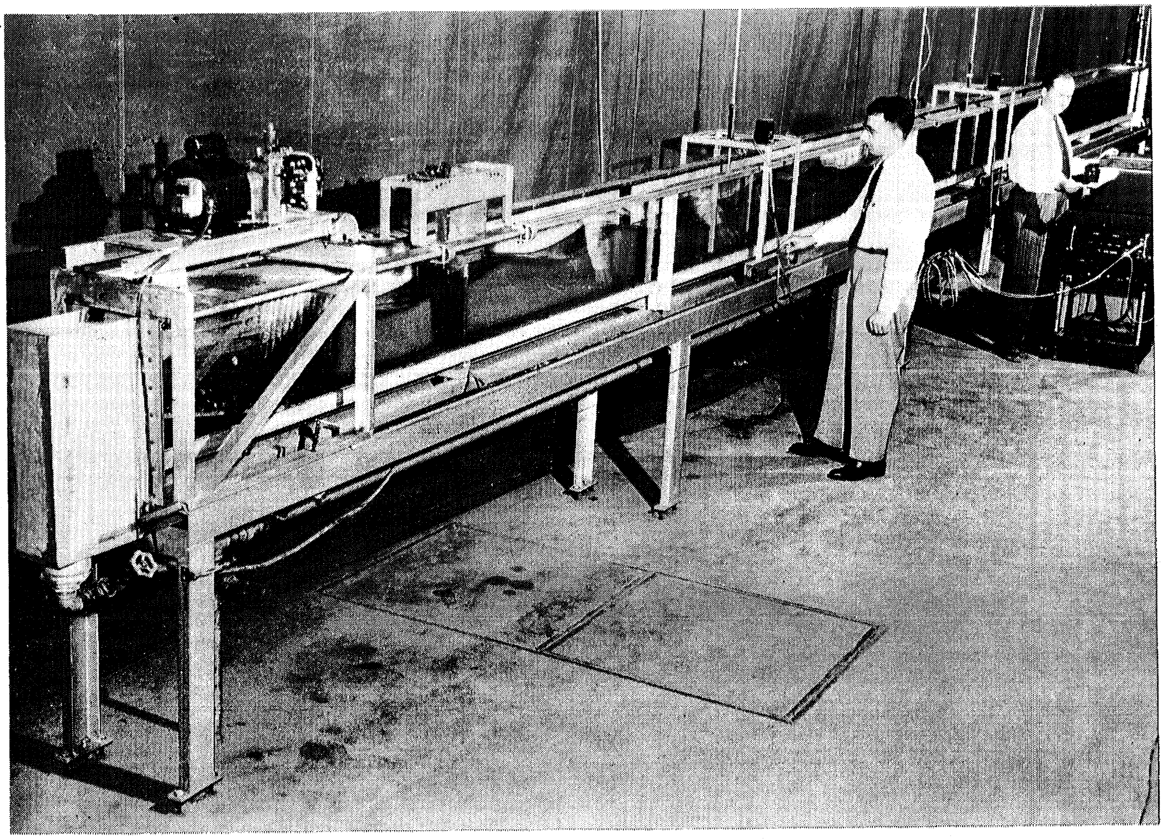

Fig. 4 - Photograph of Small Wave Channel and Equipment Used in Generation and Measuring of Waves

The test procedure consisted mainly of measuring wave attenuation for various wave lengths and jet discharges. The incident-wave height was measured at a point 8 ft upstream of the jets, and the transmitted-wave height at a point 8 ft downstream of the jets. Wave lengths of 1 to 8 ft were tested in a water depth of 12 inches. Wave steepness varied from 0.01 to 0.09 in some tests, but in general was confined to values of 0.02 or 0.04. Wave characteristics were measured with a capacitive wave-profile recorder. Air discharges were varied from 0.003 to 0.009 cfs/ft and water discharges from 0.002 to 0.012 cfs/ft.

Surface currents were measured for various discharges, depths, and distances from the breakwater utilizing a small current meter. These tests were conducted with no waves present.

C. Experimental Apparatus

1. Pneumatic Breakwater

Air bubbles were created by passing compressed air through hypodermic needles mounted on a 3/8-in. copper pipe connected by a center manifold to an air supply. Six needles were spaced at 1-in. intervals on the pipe, and each pipe was installed perpendicular to the channel walls with a 1-3/4-in. interval between pipes. Each row of jets was removable as a unit, permitting the testing of various configurations. The hypodermic needles were easily removable to allow installation of different needle sizes. Most of the tests were performed using four rows of air jets with six 26-gage standard hypodermic needles (0.008 in. ID) on each row. Air discharge was measured with a small orifice meter in the supply line.

2. Vertical Water Jets

The jets were created by forcing water through the same apparatus as used for the air bubbles, with the exception that the hypodermic needles were removed to obtain a larger jet size. A close-up view of the distributor manifold and six nozzles spaced at 1-in. intervals is shown in Fig. 5. Nozzles were used to insure parallel flow from the jets. The suction line of a centrifugal pump was attached to the lower part of the channel to obtain water for the jets, thereby maintaining a constant water depth. A single manifold pipe was used in all tests of the vertical water jets. Several different hole sizes were tested. The quantity of water was measured by means of an orifice meter in the supply line.

3. Steady Horizontal Water Jets

This type of breakwater utilized the same apparatus as that used for the vertical water jets. The entire unit was removed from the channel bed and placed perpendicular to the channel walls in a horizontal position, with the jets opposing the direction of wave propagation (Fig. 6). The unit was submerged 1 in. below the still-water level, this depth being sufficient to prevent the jets from issuing into the air as the wave trough passed the manifold. The jets were parallel to the still-water surface. A single manifold pipe was used for all tests of the horizontal water jets described in this report.

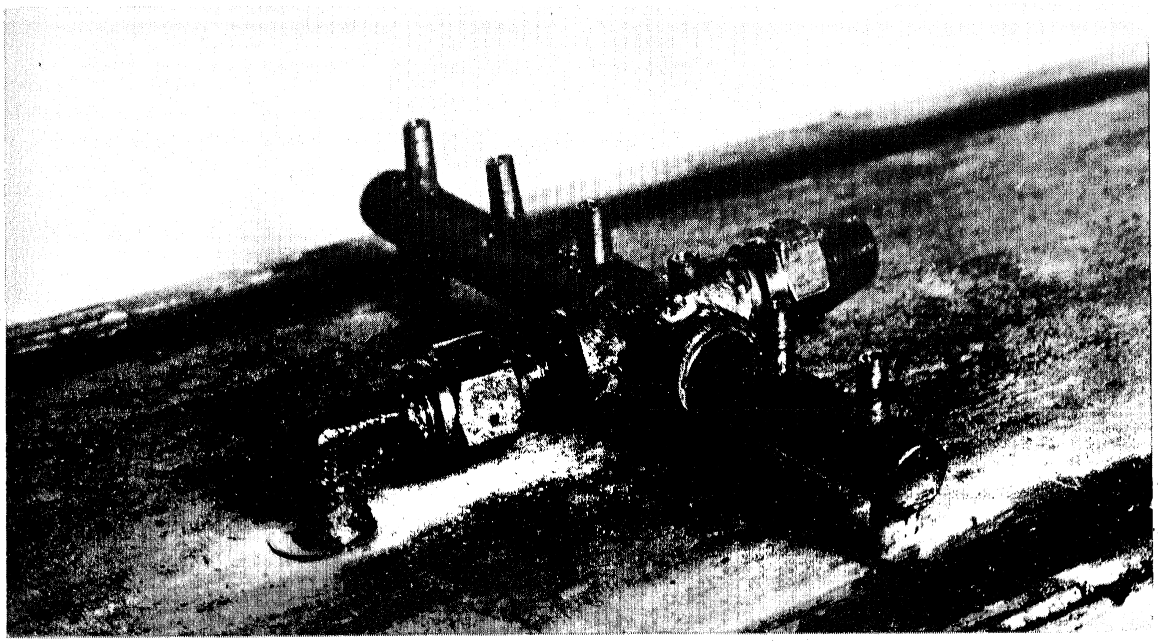

Fig. 5 - Photograph of Vertical Water-Jet Manifold Pipe

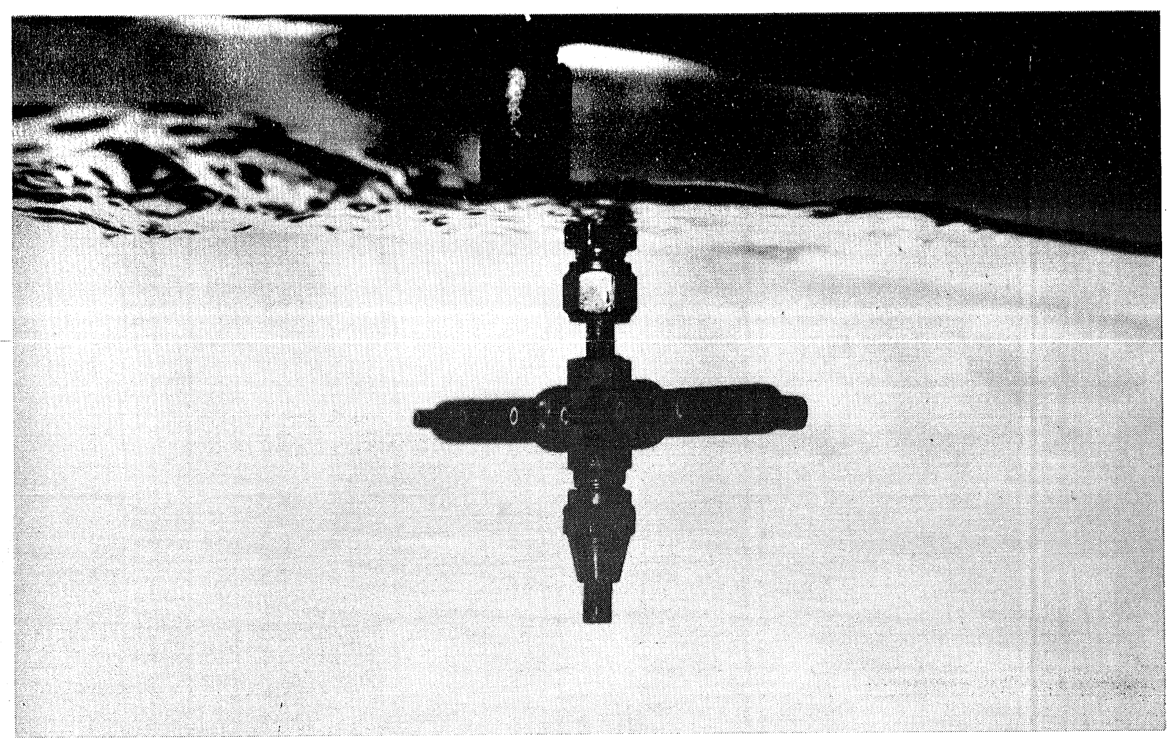

Fig. 6 - Photograph of Horizontal Water-Jet Manifold Pipe

4. Pulsating Horizontal Water Jets

The horizontal jet manifold and nozzles were left in the same position for this study. A solenoid valve was placed in the supply line to pulsate the jets. This valve was operated by a relay controlled by a microswitch. A cammed disc was attached to a shaft from the wave-generator hydraulic-drive unit. The contact arm of the microswitch rode on the disc and its movements were controlled by the cammed portion of the disc. It was found that such a device gave the necessary control over the pulsations. By proper adjustments the pulsations could be set at any phase relationship with respect to the incident-wave period or multiple thereof. The quantity of flow was measured with a calibrated water meter in the supply line.

V. DISCUSSION OF EXPERIMENTAL RESULTS

A. Surface Current Study

The strength of the surface current induced by the various breakwaters, and particularly by the pneumatic breakwater, was of interest in an attempt to correlate the data with the theory proposed by Taylor. It was found that the induced current was not steady, and an average of several readings was required to provide consistent results. Some typical velocity profiles at specified distances from the jets for two different discharges are shown in Fig. 7. From these plots one can see immediately that the current is stronger near the surface, with the magnitude diminishing rapidly with depth. The profiles qualitatively verify the predicted profiles of Fig. 2.

The volume of air required to produce a given surface current was computed from Taylor's theory, Eq. (14), described in Section III and plotted in Fig. 8. The experimental points agree well with the theory for the range of discharges tested. This curve illustrates the large discharge increment necessary to increase the magnitude of the surface current.

The hydraulic jets produced a velocity profile very similar to that caused by the rising air bubbles. Some typical profiles created by vertical jets are shown in Fig. 9 and by horizontal jets in Fig. 10. It is evident that the horizontal jets create a much stronger surface current than the vertical jets. With the horizontal jets, nearly all the energy is available for developing the upstream surface current, the symmetrical downstream surface

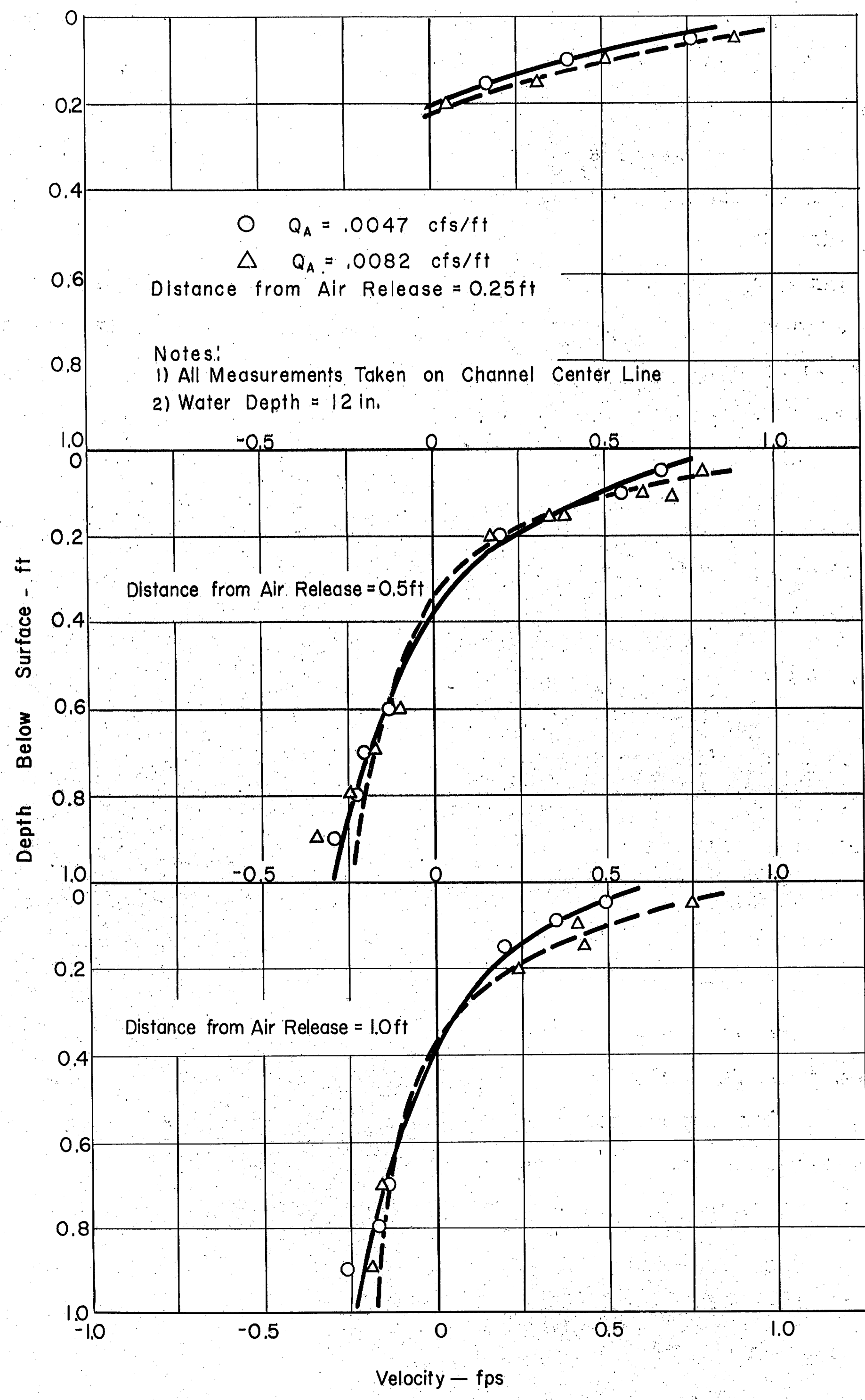

Fig. 7 - Water Currents Produced by a Pneumatic Breakwater

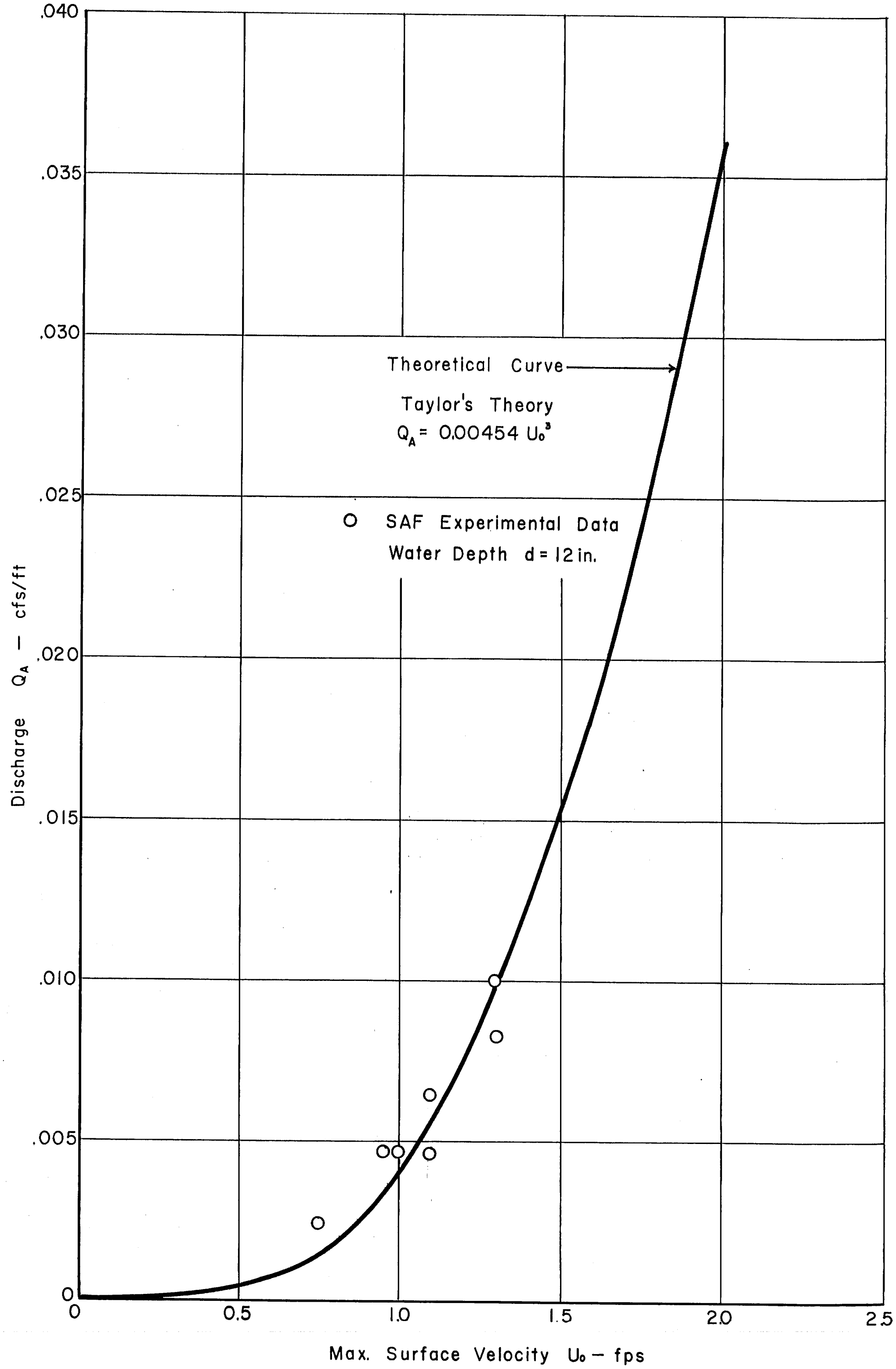

Fig. 8 – Comparison of Theoretical and Experimental Surface Current Velocities Produced by Pneumatic Breakwater

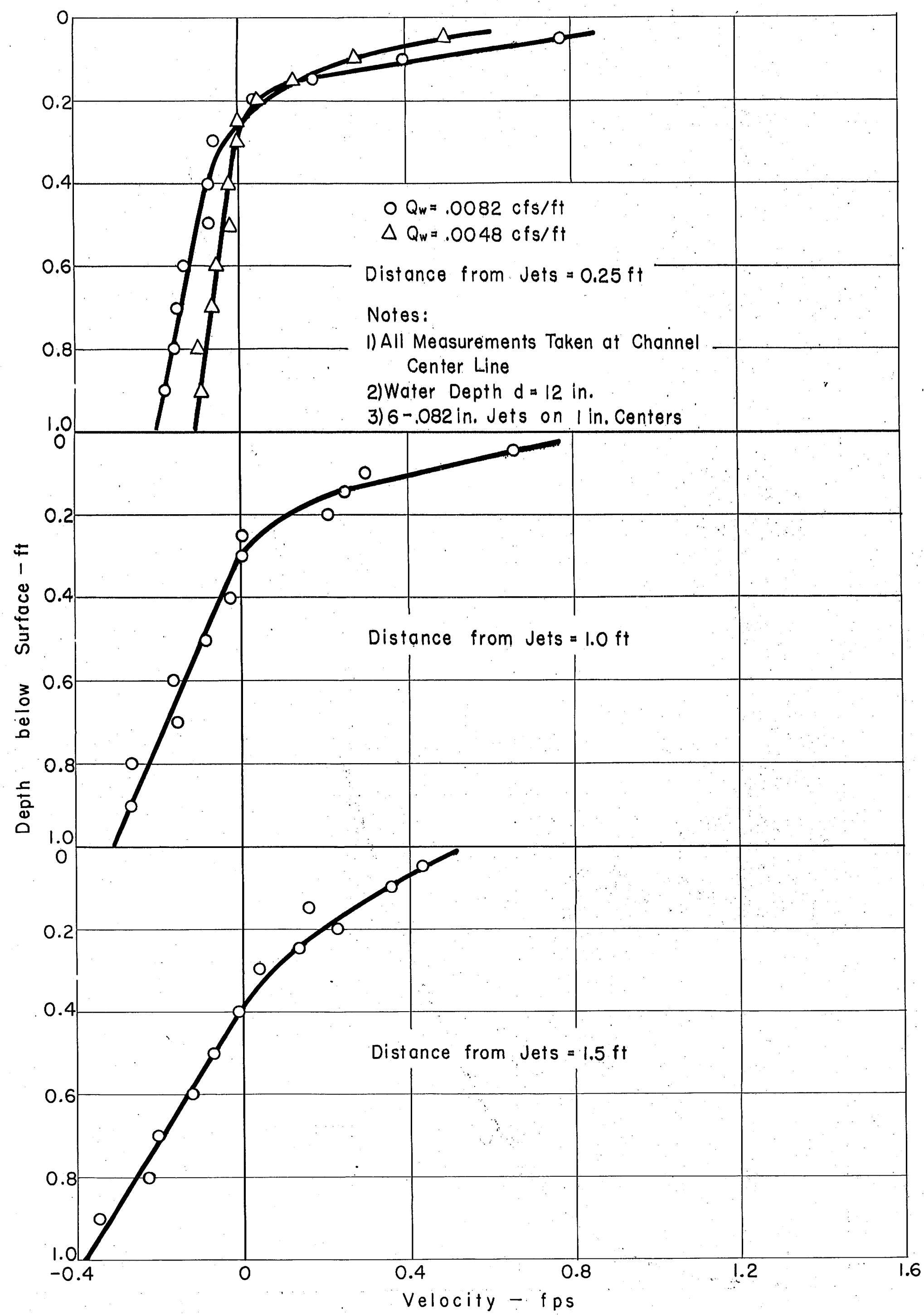

Fig. 9 – Water Currents Produced by Vertical Water Jets

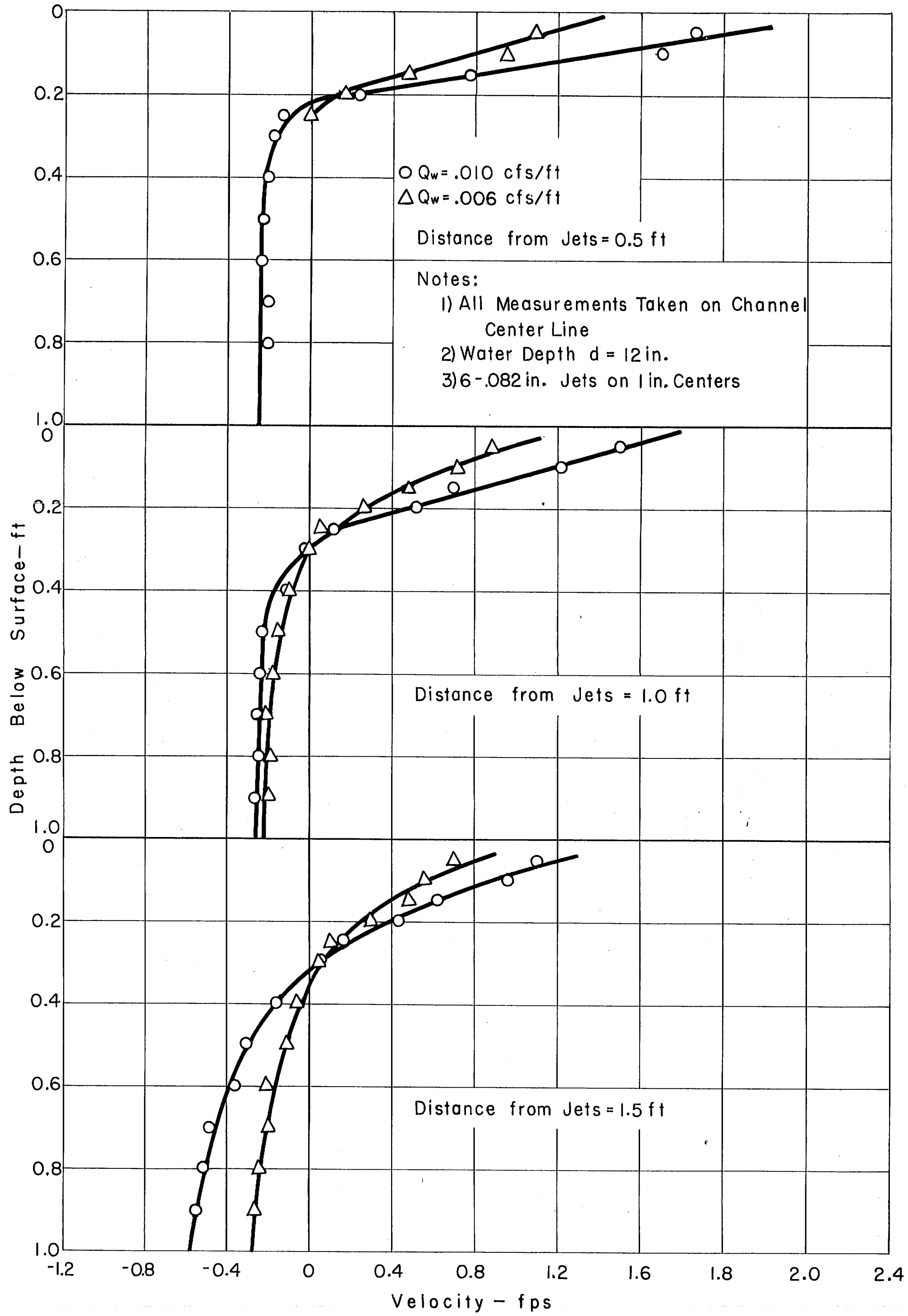

Fig. 10 – Water Currents Produced by Horizontal Water Jets

current not being created. A comparison of typical profiles for the two jet positions is shown in Fig. 11 for approximately the same discharges. Theoretically, the positive and negative portions of the velocity profiles should be equal. The error that existed here was attributed to the small scale at which these tests were run, but in any case, the profile presented a basis for comparison of the jet arrangements. As the maximum depth of the opposing current extends to about 0.3 ft, the profiles indicate that the surface current will have little effect on shallow-water waves whose particle motion extends to the bottom. Additional surface current data are tabulated in Appendix A.

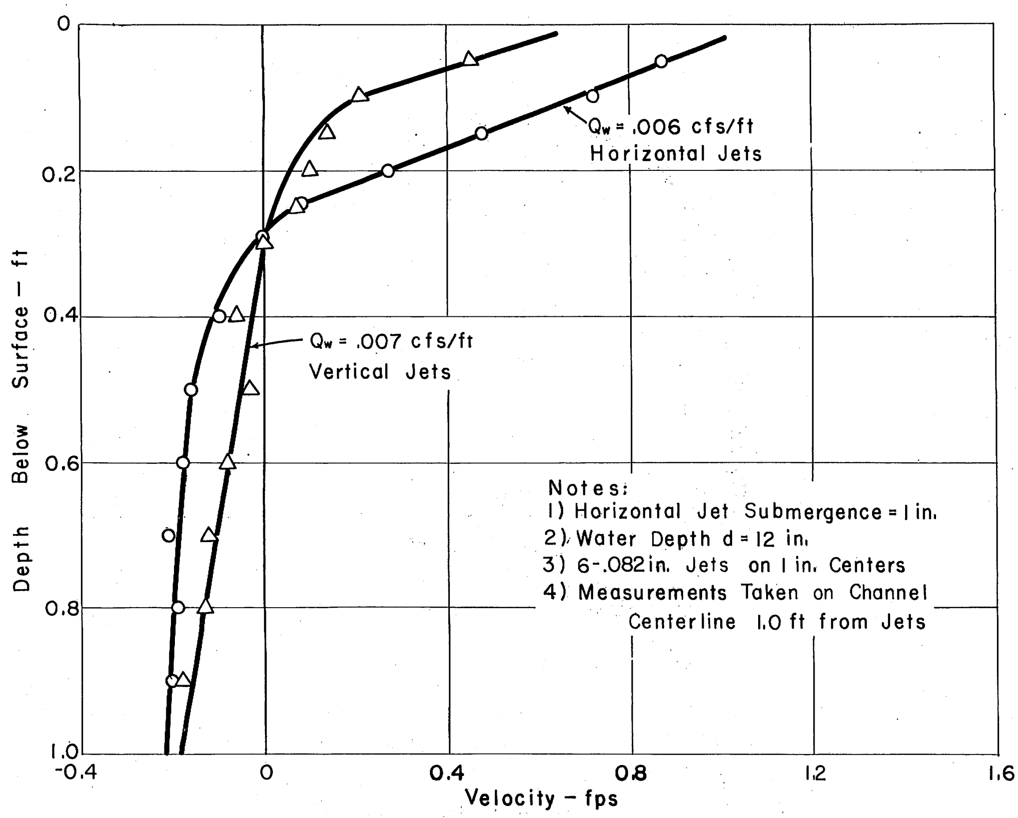

Fig. 11 – Comparison of Surface Currents Produced by a Water-Jet Breakwater

B. Breakwater Performance

Figure 12 illustrates the effectiveness of the pneumatic breakwater. The device is reasonably effective for deep-water waves, but for the shallow-water waves the breakwater has little effect. The graph also indicates that for a constant water depth a limit exists on the length of wave that can effectively be attenuated. The discharges shown are not the maximum obtained, but were used to illustrate typical conditions.

The agreement with Carr's data is qualitative, in that a similar shape of curve was obtained, and the data are an extension of his work in the region of L/d < 2. Carr used from one to five distributor pipes permitting a discharge of 0.033 to 0.166 cfs/ft. This is about 5 to 25 times the discharge for the St. Anthony Falls Hydraulic Laboratory data. In both cases, the data have some scatter, probably because of the instability of the breakwater itself.

If different discharges are selected, a series of curves will result that parallel--in the lower L/d region--those of Fig. 12. These curves are plotted in Fig. 13 and illustrate the typical shape of the curves. The curves of constant discharge can also be considered as curves of constant horsepower, and values of attenuation for any particular horsepower and L/d can easily be determined.

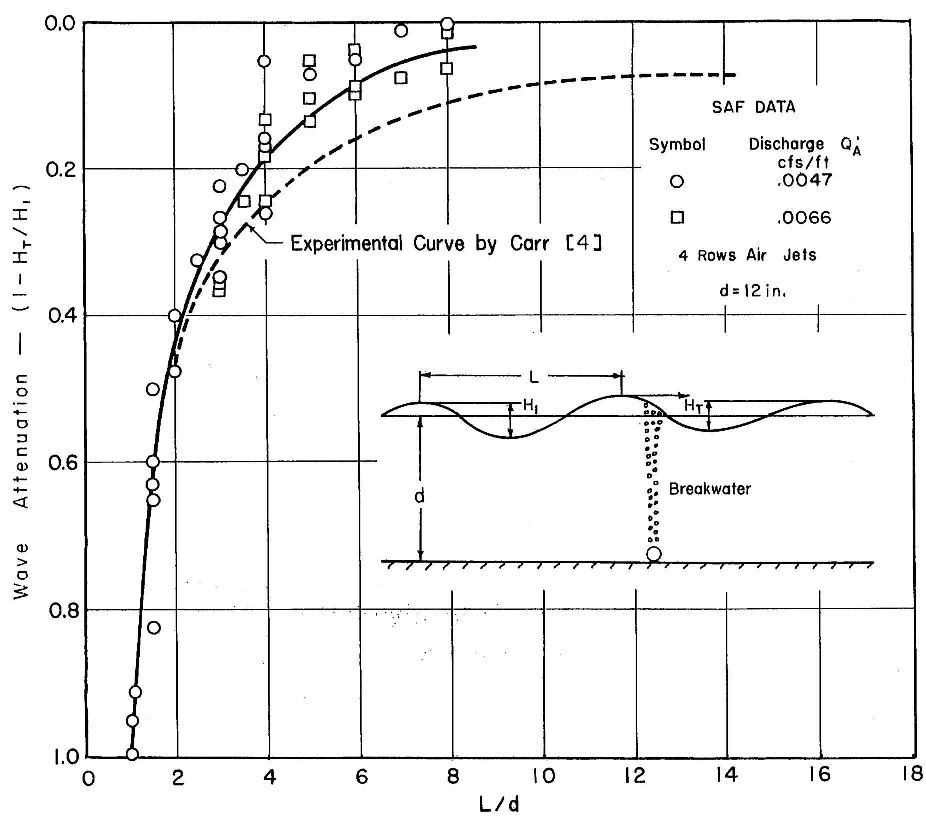

Fig. 12 - Comparison of Carr's Data with SAF Data for Pneumatic-Breakwater Performance

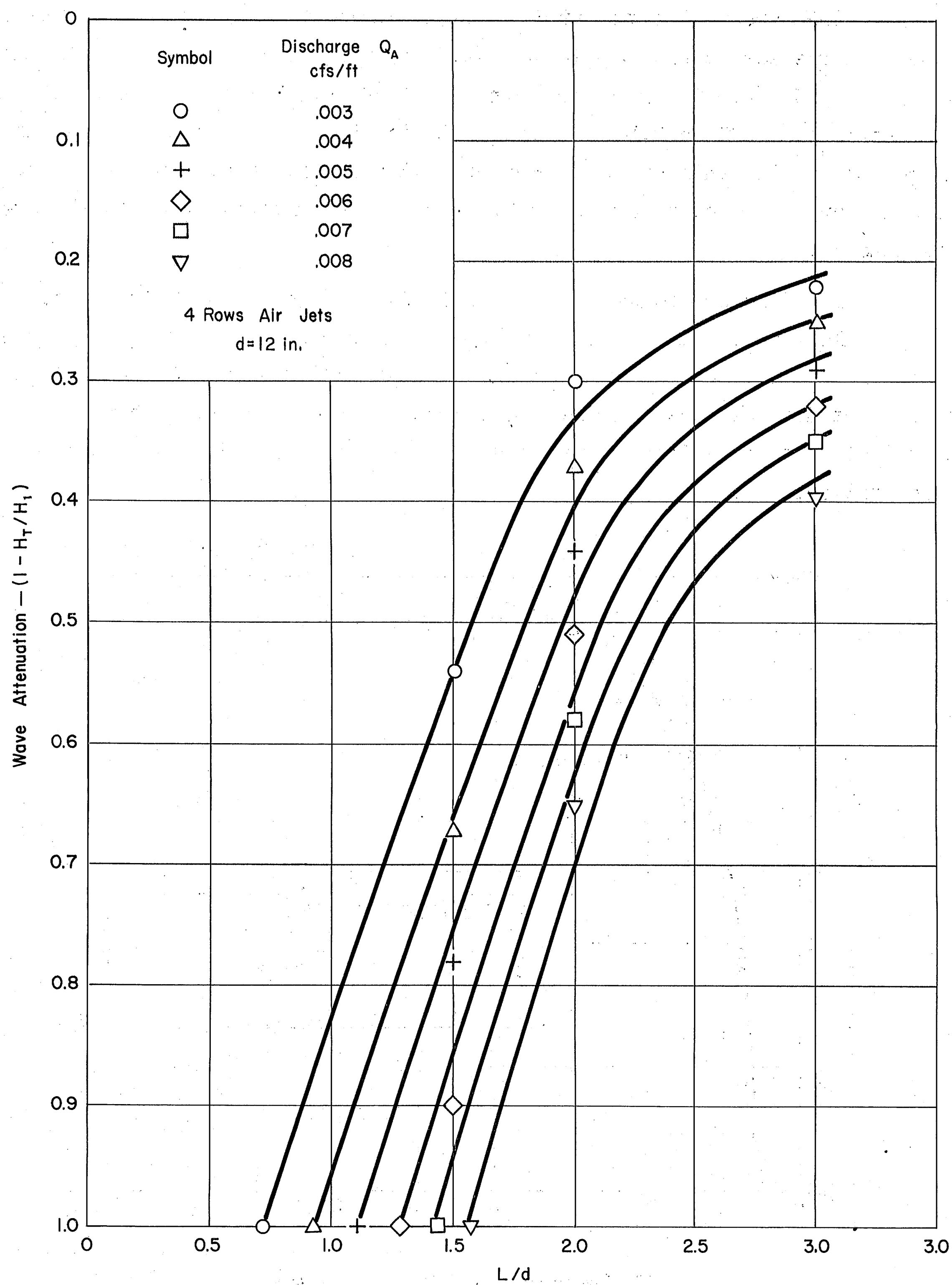

Fig. 13 – Effect of L/d on Wave Attenuation for Various Discharges of Pneumatic Breakwater

The performance of the water jets is shown in Fig. 14. The curves are similar in shape to those of Fig. 12 and indicate that the water jets are also not effective in attenuating waves of large L/d. The effectiveness of the vertical jets is lower than that of the horizontal jets, probably caused by the fact that for equal discharges the horizontal jets induce a much greater surface current.

As with the pneumatic breakwater, the curves can be considered as curves of constant horsepower rather than discharge, and by changing the discharge a series of curves can be drawn similar to those in Fig. 13.

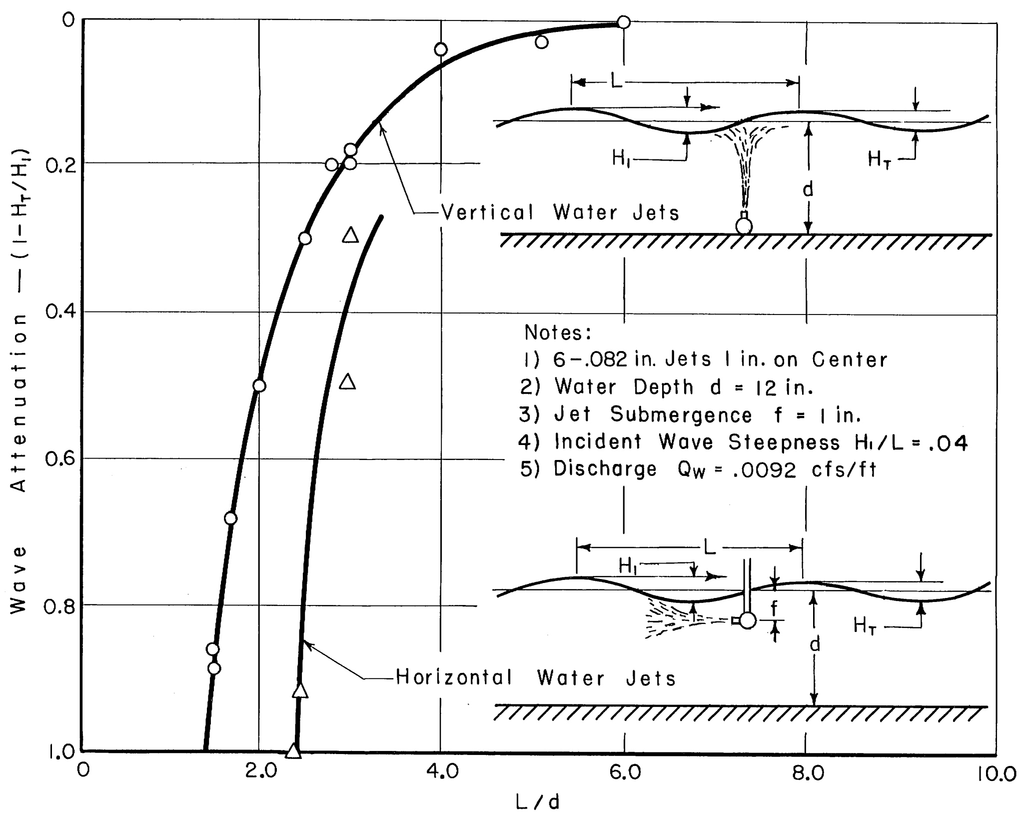

Fig. 14 - Water-Jet Breakwater Performance

The maximum values of L/d achieved in the tests are given in Table II. These values could have been increased by providing for larger discharges, but this was not considered justified as the horsepower requirements appeared to be quite high.

TABLE II

Attenuation	Maximum L/d Achieved in Tests		
	Pneumatic	Horizontal Water Jet	Vertical Water Jet
90	1.65	2.45	1.5
70	2.00	2.55	1.7
50	2.37	2.75	2.0

C. Effect of Discharge on Attenuation

As previously noted, an increase in discharge will result in an increase in the magnitude of the induced-surface current, which will cause an increase in wave attenuation of deep-water waves. The typical photographs of the vertical water jet in Fig. 15 show for a constant discharge (Q_W = 0.0082 cfs/ft) attenuation as a function of wave length. The wave length was varied from 1.5 to 3.0 ft with a wave steepness of 0.04. Some typical photographs of the horizontal water jet (Fig. 16) show that for approximately the same discharge the 2.5-ft wave was almost completely stopped, indicating that a strong surface current is required for efficient attenuation.

It was found that as the jet discharge and consequently the strength of the surface current increased, the wave length shortened as the waves entered the current region. The wave steepness increased, and the wave crest became very unstable as it approached the point of breaking. Figure 17 illustrates the instability of the wave crest for L = 2.0 ft and two different discharges of the horizontal water jet. For short waves and high jet discharges, a lateral instability developed, which in some instances made measurements difficult.

In general, increasing the discharge increased the attenuation of a deep-water wave of given L/d until it was eventually stopped. Figures 18, 19, and 20 show this effect for the pneumatic and hydraulic breakwaters. (Also see Figs. A-1 and A-2 in Appendix A.) It is evident that the longer waves require a much higher discharge than the shorter waves to achieve a specified attenuation. A comparison of the discharge requirements for vertical and

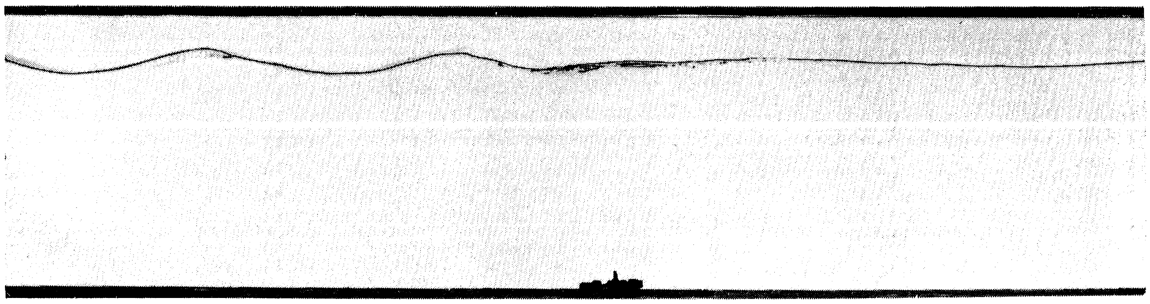

a. L = 1.5 ft   Attenuation = 70%

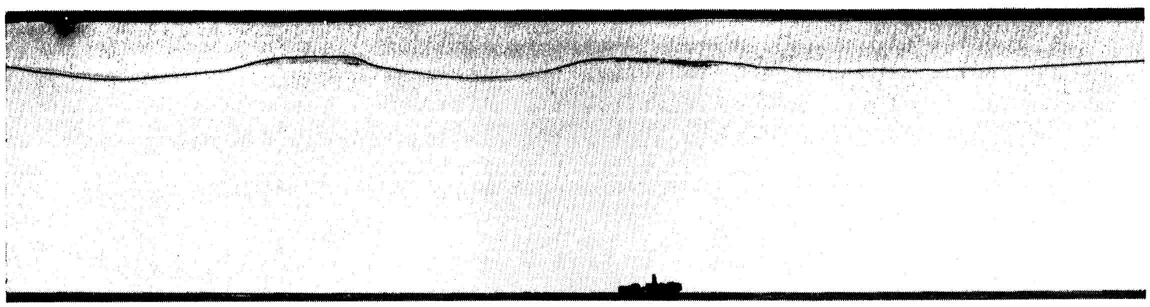

b. L = 2.0 ft   Attenuation = 42%

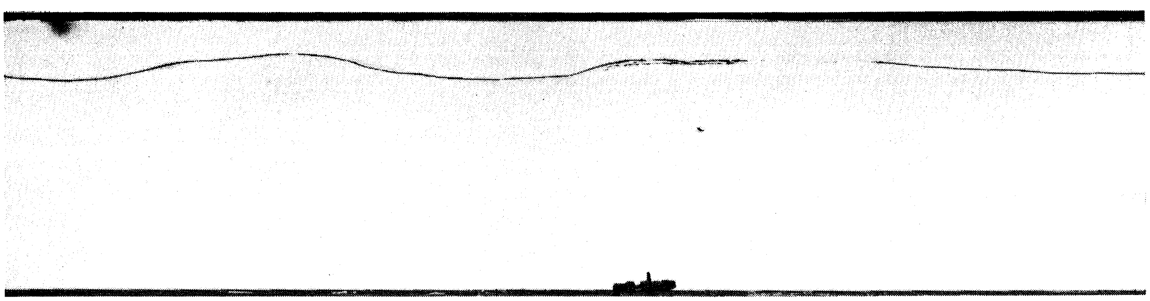

c. L = 2.5 ft   Attenuation = 30%

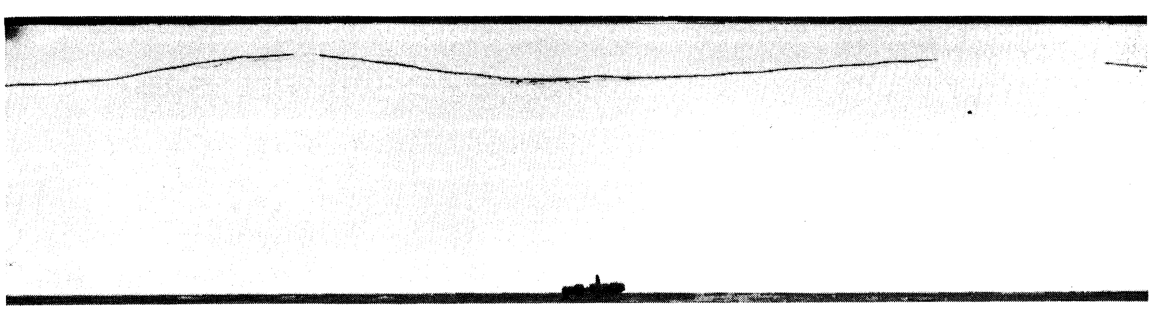

d. L = 3.0 ft   Attenuation = 20%

Fig. 15 – Photographs Showing Attenuation by Vertical Water Jets
Q_W = 0.0082 cfs/ft, H_I/L = 0.04

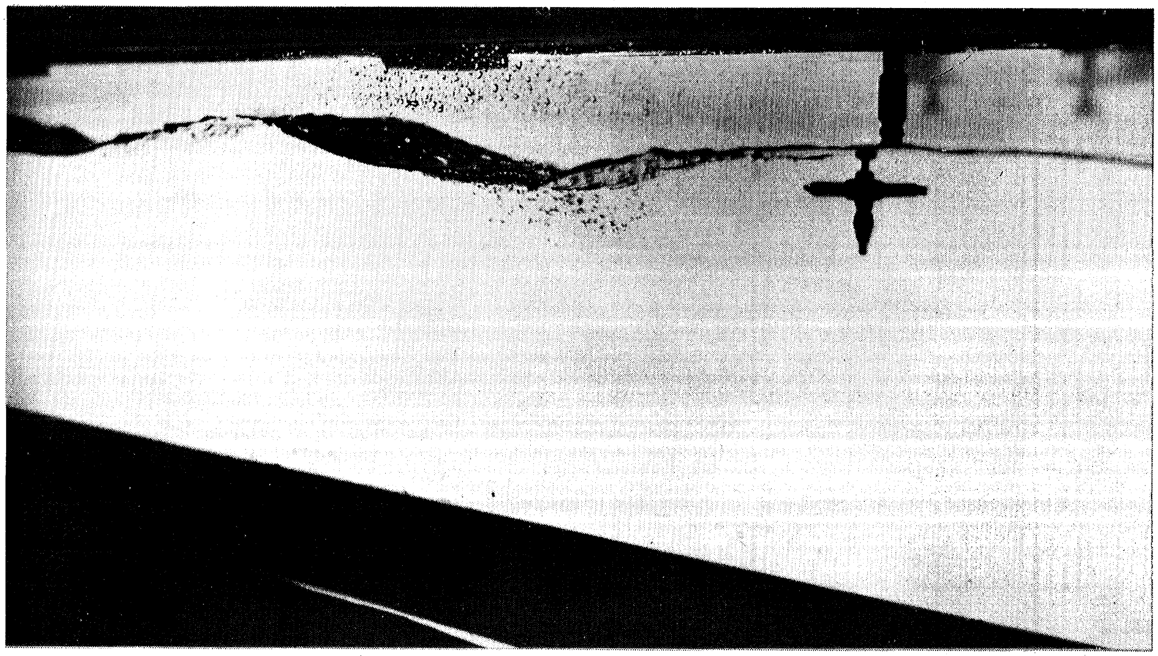

a. L = 3.0 ft   Attenuation = 50%

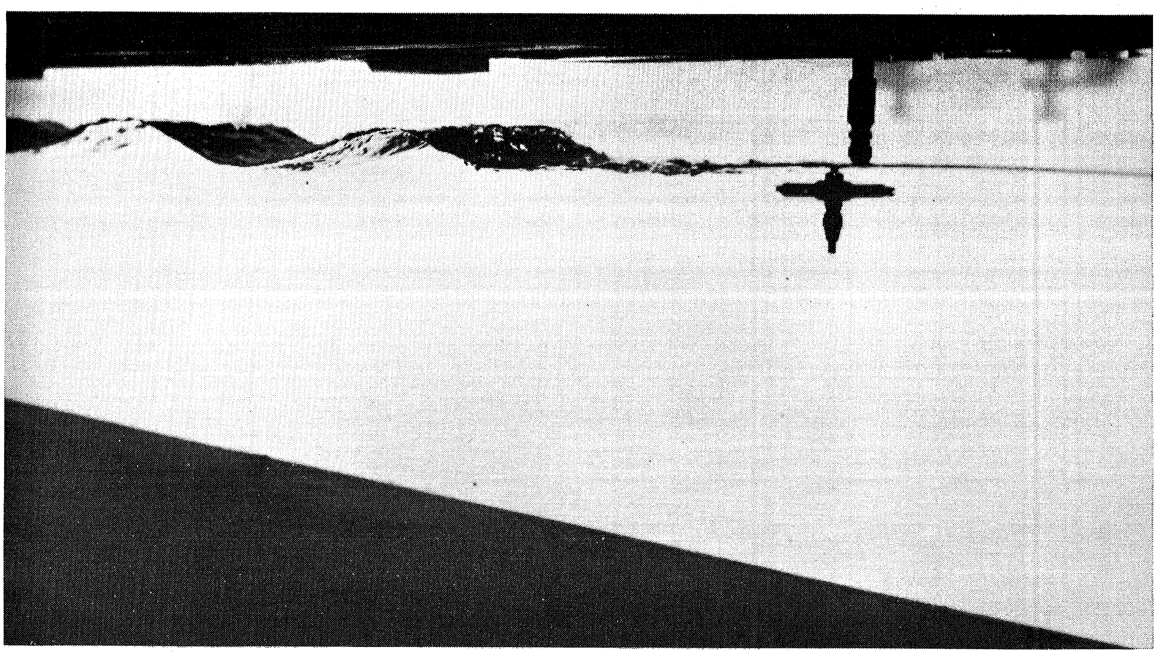

b. L = 2.5 ft   Attenuation = 100%

Fig. 16 – Photographs Showing Attenuation by Horizontal Water Jets
Q_W = 0.0088 cfs/ft, H_I/L = 0.04

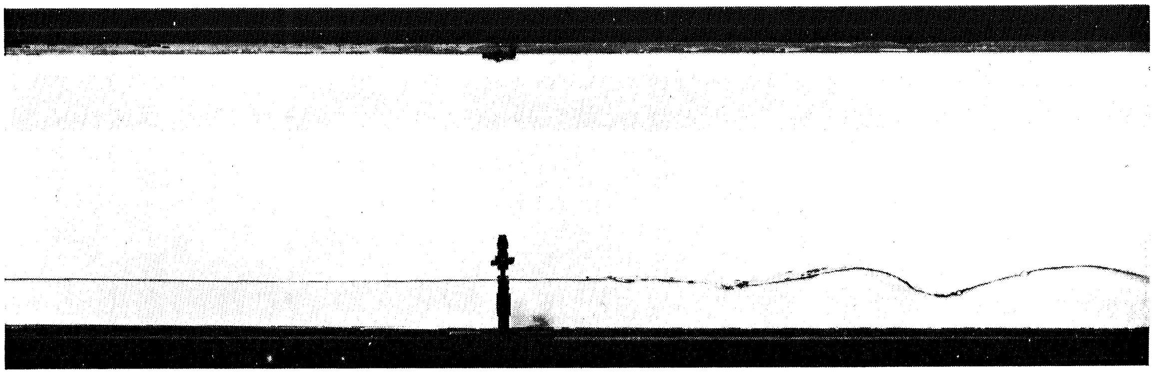

a. L = 2.0 ft Q_w = 0.0075 cfs/ft Attenuation = 100%

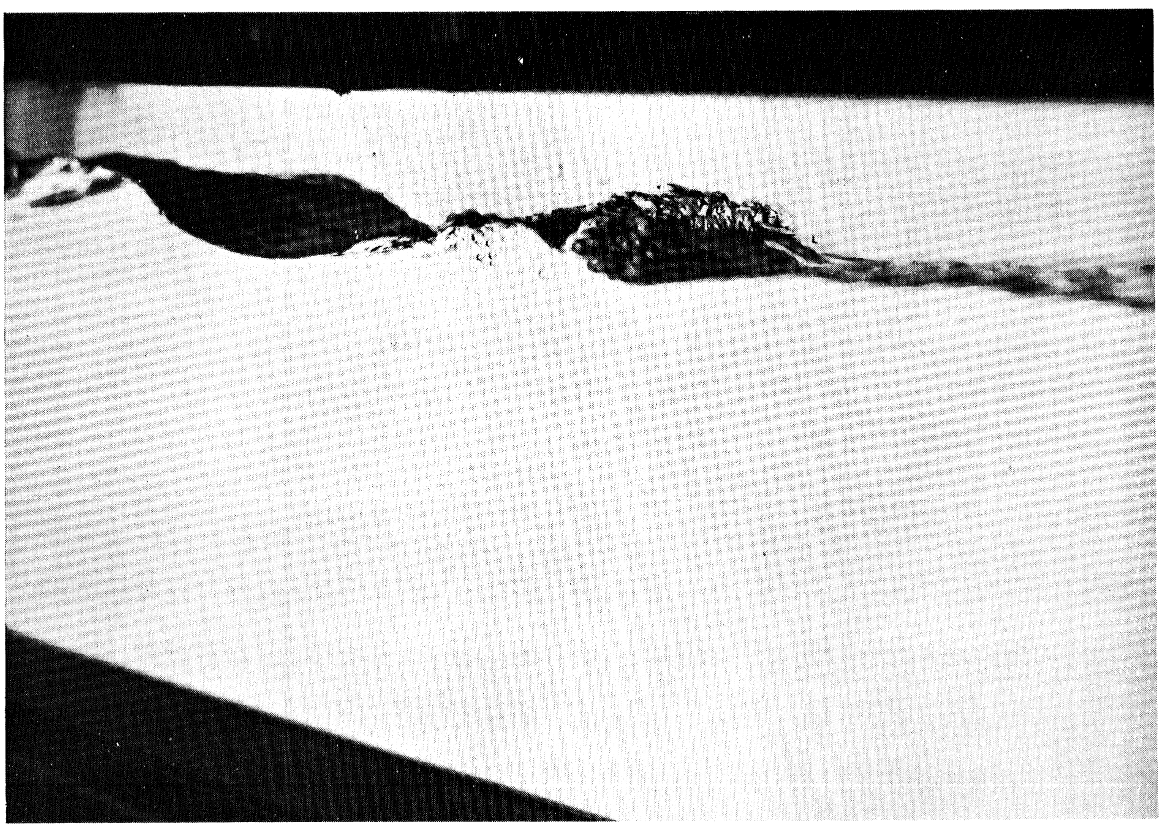

b. L = 2.0 ft Q_w = 0.0085 cfs/ft Attenuation = 100%

Fig. 17 - Wave Crest Instability Created by Horizontal Water Jets
H_I/L = 0.06

horizontal water jets is shown in Fig. 21, where the greater effectiveness of the horizontal jets can be seen immediately. For example, if a 2-ft wave is to be attenuated 50 per cent, the vertical jet requires approximately one and one-half times the discharge of the horizontal jet for this particular jet diameter. On an energy basis, the vertical jet requires about five times the energy of the horizontal jet for a given wave and attenuation. It thus appears that the horizontal jet is more efficient than the vertical jet in absorbing waves.

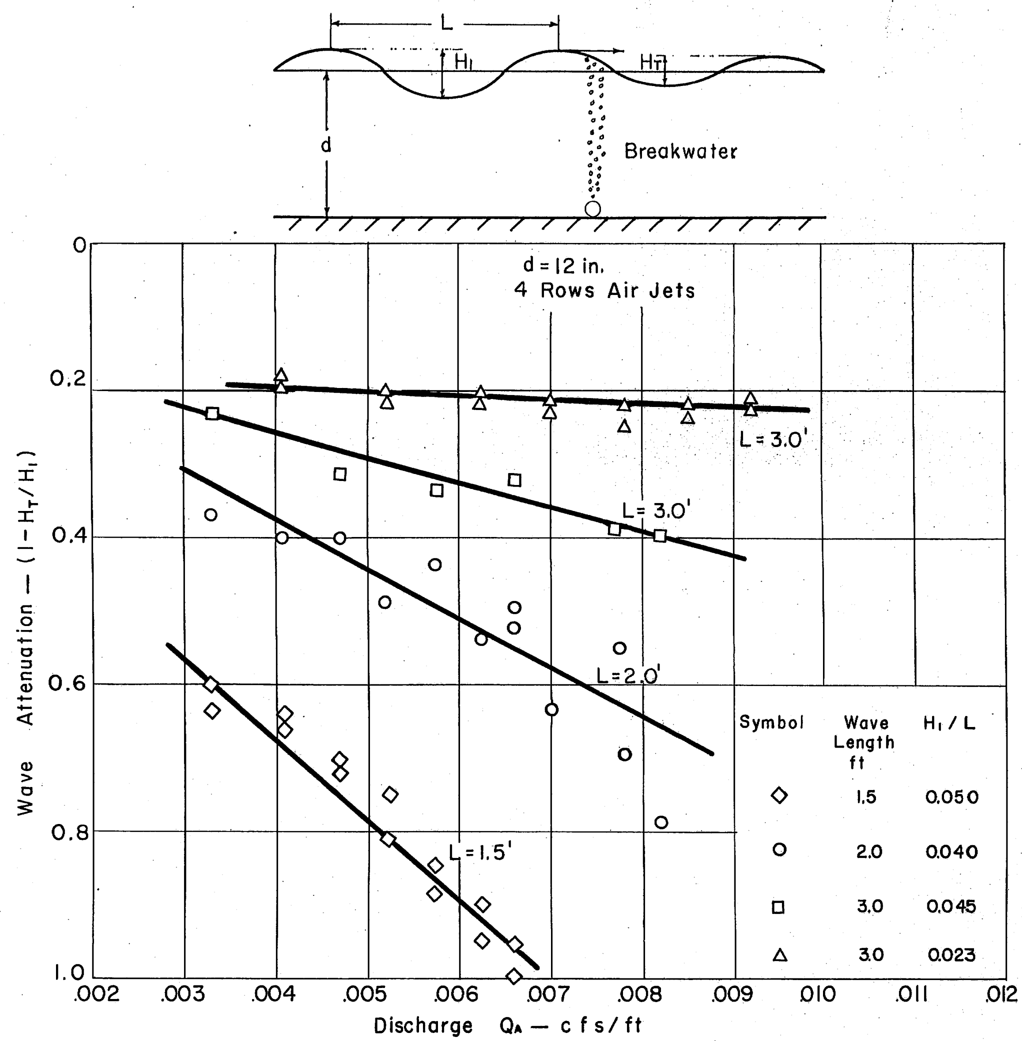

Fig. 18 – Effect of Air Discharge on Wave Attenuation

With either of the jet types, pneumatic or hydraulic, the curves are relatively flat for the longer waves (such as L/d = 3). This shows that for the particular types of jet arrangements considered, discharge has little effect on wave attenuation in the shallow-water wave region. The current profiles of Section V-A indicated that the opposing current is confined to a region near the surface. It appears that an opposing current extending over a larger portion of the water depth is necessary to effectively attenuate the longer waves. With the pneumatic and the vertical water jets, this can perhaps be accomplished by increasing the submergence of the manifold pipes, although a limiting position is finally reached. The horizontal water jet

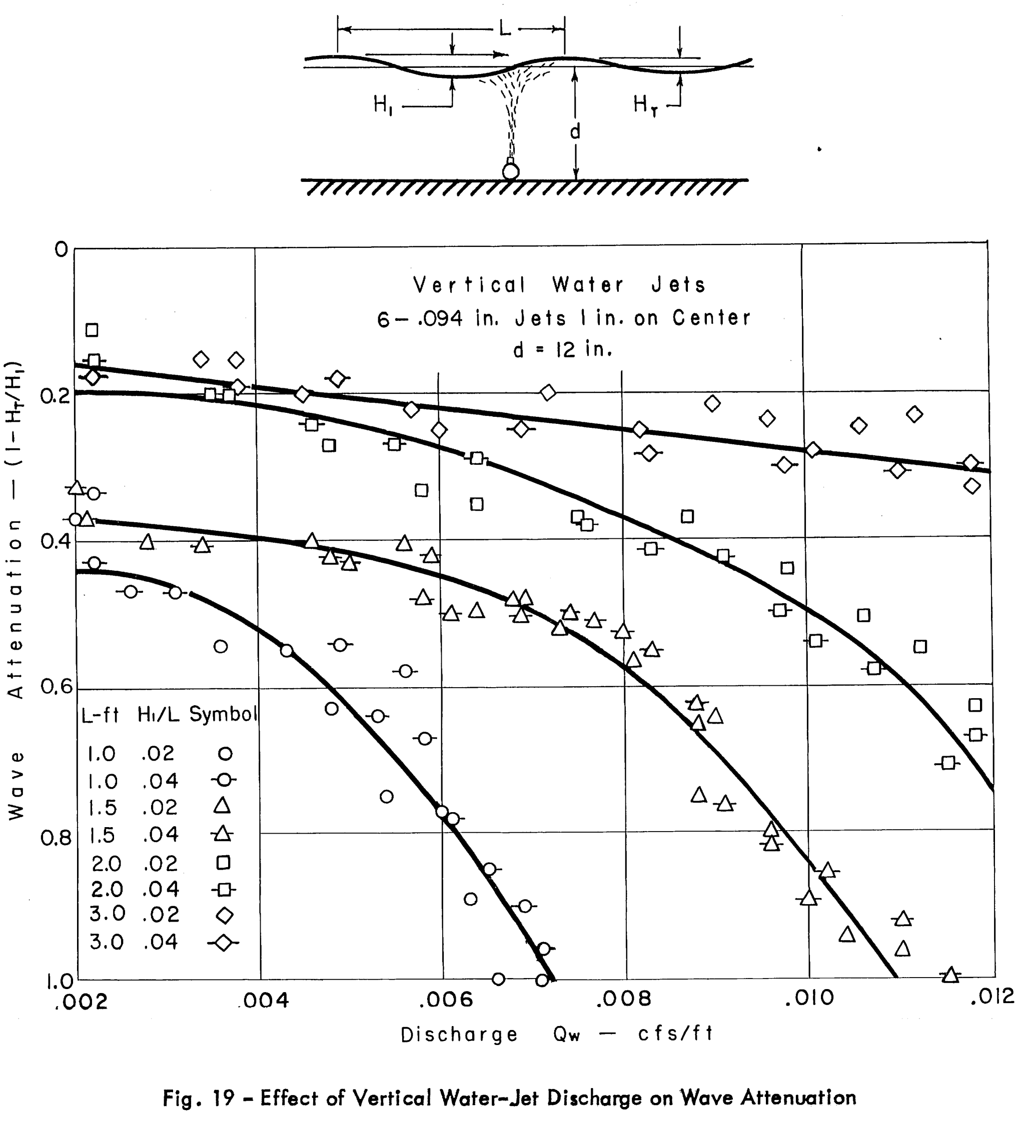

Fig. 19 – Effect of Vertical Water-Jet Discharge on Wave Attenuation

can most easily be utilized for increasing the depth of the current. Several rows of manifold pipes can be added, and nearly any desired current depth can be obtained, provided sufficient horsepower is available for such an operation.

From one to four manifold pipes were used in the tests of the pneumatic breakwater. It was found that the number of pipes had little significant effect on wave attenuation for the range of conditions covered in this investigation. The effectiveness of the breakwater for a constant discharge

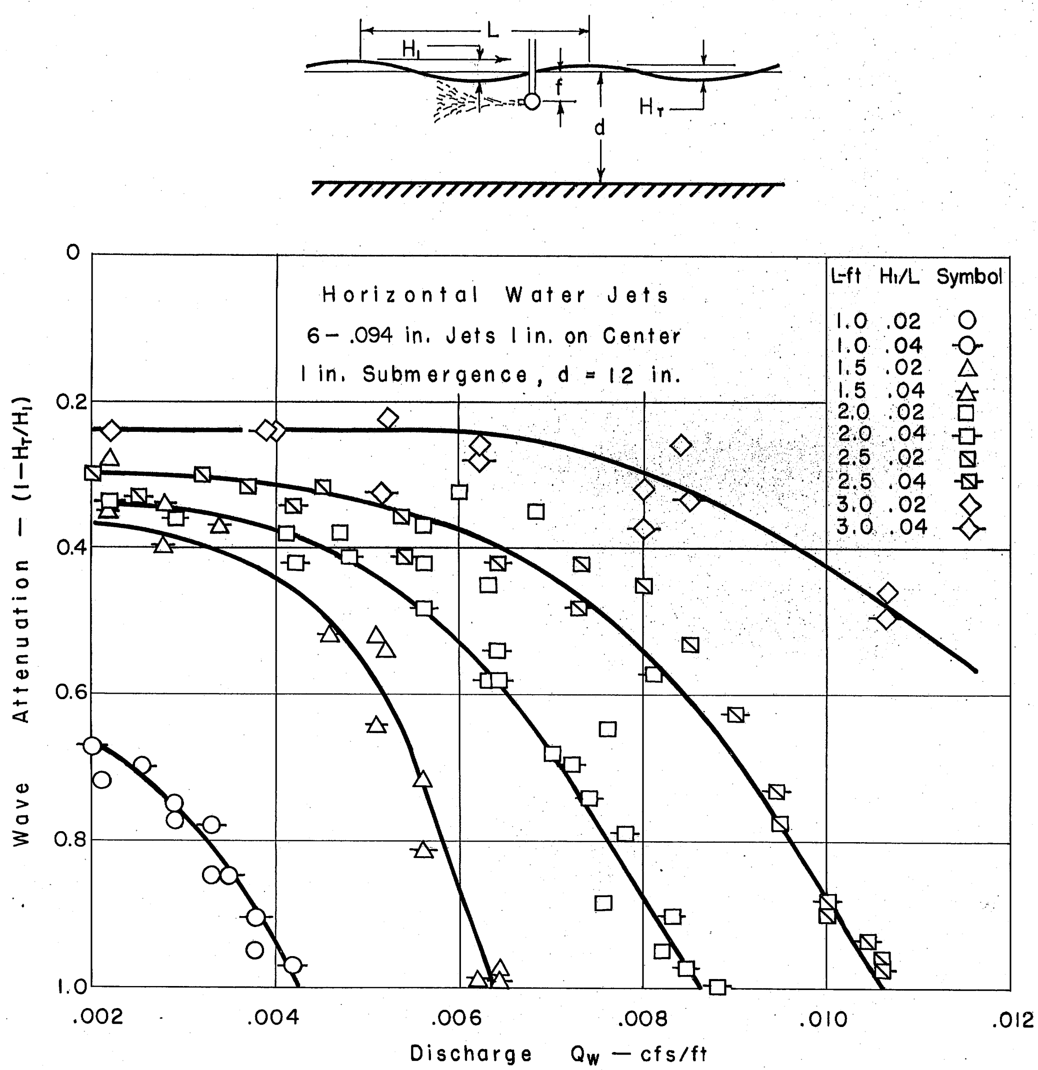

Fig. 20 – Effect of Horizontal Water-Jet Discharge on Wave Attenuation

appeared to increase slightly as the number of manifold pipes increased. This may be caused by an effect of spacing. However, the data had considerable scatter and were not sufficient to determine the effect completely.

A short study was made with the horizontal jets pointing downstream in the direction of wave propagation. It was observed that the current had a tendency to flatten or temporarily dampen the waves in the current region. After leaving this region, the waves again began to recover some of their original height. In any case, the current had relatively little effect on wave attenuation, indicating that a surface current flowing against the waves is necessary for efficient absorption.

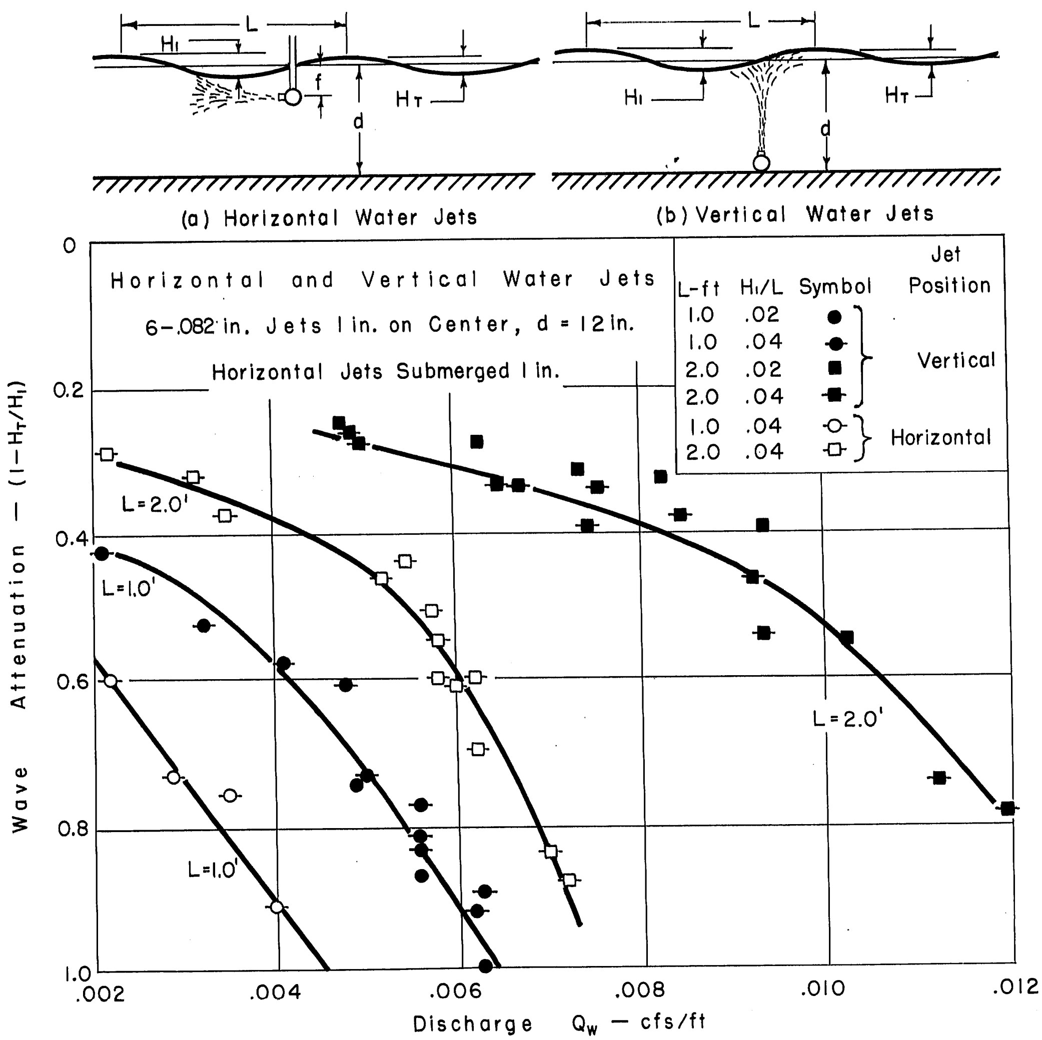

Fig. 21 - Comparison of Horizontal and Vertical Water-Jet Discharges

D. Effect of Wave Steepness on Attenuation

The theory by Taylor described in Section III did not consider wave height as a parameter. Therefore, any computation made is independent of wave height. Some work by Carr and also by Yi-Yuan-Yu [7] indicates that attenuation is largely dependent on the ratio of uniform-current velocity to the wave celerity. Since wave celerity is primarily dependent on wave length and water depth, it appears that wave height should have a minor effect on attenuation. The effect of wave steepness was investigated, and the results obtained from the tests of the pneumatic breakwater (Fig. 22) indicated that variations in wave steepness from 0.02 to 0.09 did not produce significant

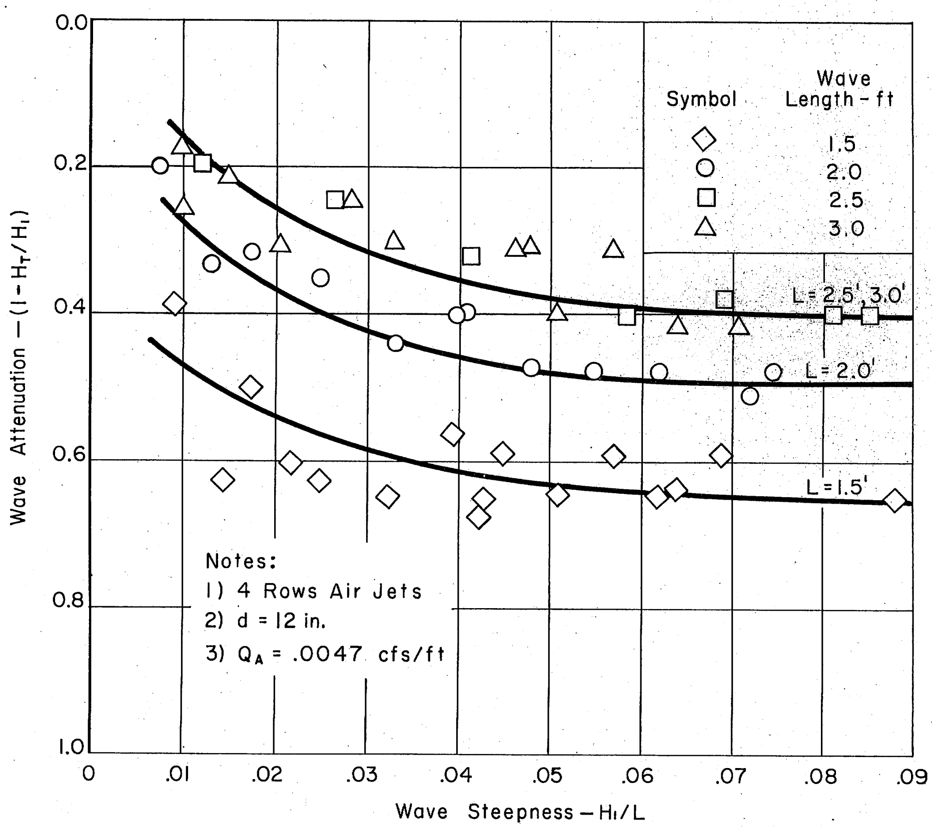

Fig. 22 – Attenuation as a Function of Wave Steepness (H_I/L) for Pneumatic Breakwater

variations in attenuation. A similar effect was also noted in tests with the horizontal water jets (Fig. 23) for two different discharges. However, the data are not sufficient to completely determine the effect. Other wave lengths and jet discharges should be investigated. It was difficult in the small channel to generate stable waves of the desired length with H_I/L less than 0.02 or greater than 0.09. For values of wave steepness below 0.02, particularly below 0.01, or for values above 0.09, significant variations in attenuation may exist.

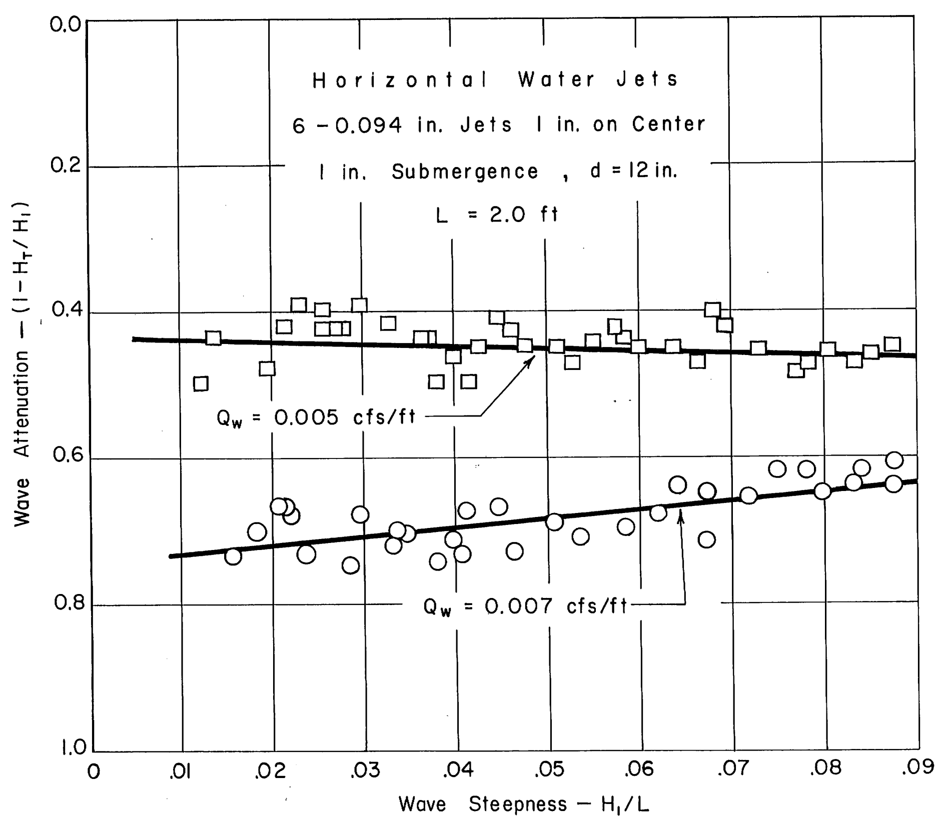

Fig. 23 - Attenuation as a Function of Wave Steepness H_I/L for Hydraulic Breakwater

E. Effect of Jet Submergence on Attenuation

The effect of jet submergence for the horizontal jets is shown in Fig. 24. The entire apparatus was lowered, increasing the mean submergence from 1 in. to 2 inches. As one might expect, the attenuation for a given wave length and discharge was considerably less for the greater submergence, indicating that a strong-surface current is a requirement for most effective attenuation of deep-water waves. The upper limit of submergence was chosen to prevent the jets from issuing into air when the wave trough passed over the jet apparatus. Referring to Fig. 24 for an 80 per cent attenuation of a 2-ft wave, a discharge of 0.007 cfs/ft is required for a 1-in. submergence, whereas a discharge of 0.0083 cfs/ft is required for a 2-in. submergence, an increase of about 19 per cent for this wave length and attenuation.

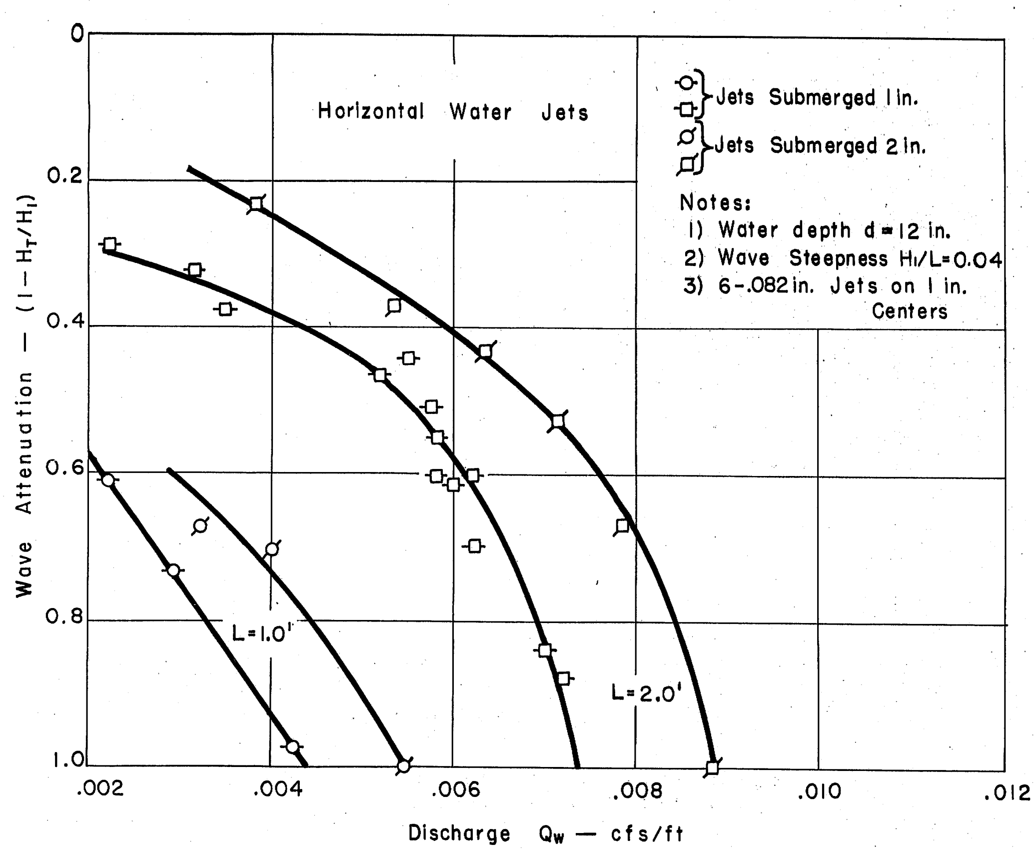

Fig. 24 - Effect of Horizontal Water-Jet Submergence on Wave Attenuation

F. Effect of Jet Diameter on Attenuation

In an attempt to reduce the jet energy $(V_j^2/2g)$ for a specified wave length and attenuation, the diameter of the jets was increased. The effect of jet diameter as a function of attenuation and discharge is shown in Fig. 25. It is evident that the larger diameter requires a larger discharge to attenuate the wave. If one considers the power requirements of each jet for an 80 per cent attenuation, the 0.094-in. diameter requires minimum power, this diameter being perhaps the most efficient hole size. The effect of jet spacing may also be an important parameter. Studies of this type were not conducted in the small channel, but will be investigated in the 9-ft wave tank.

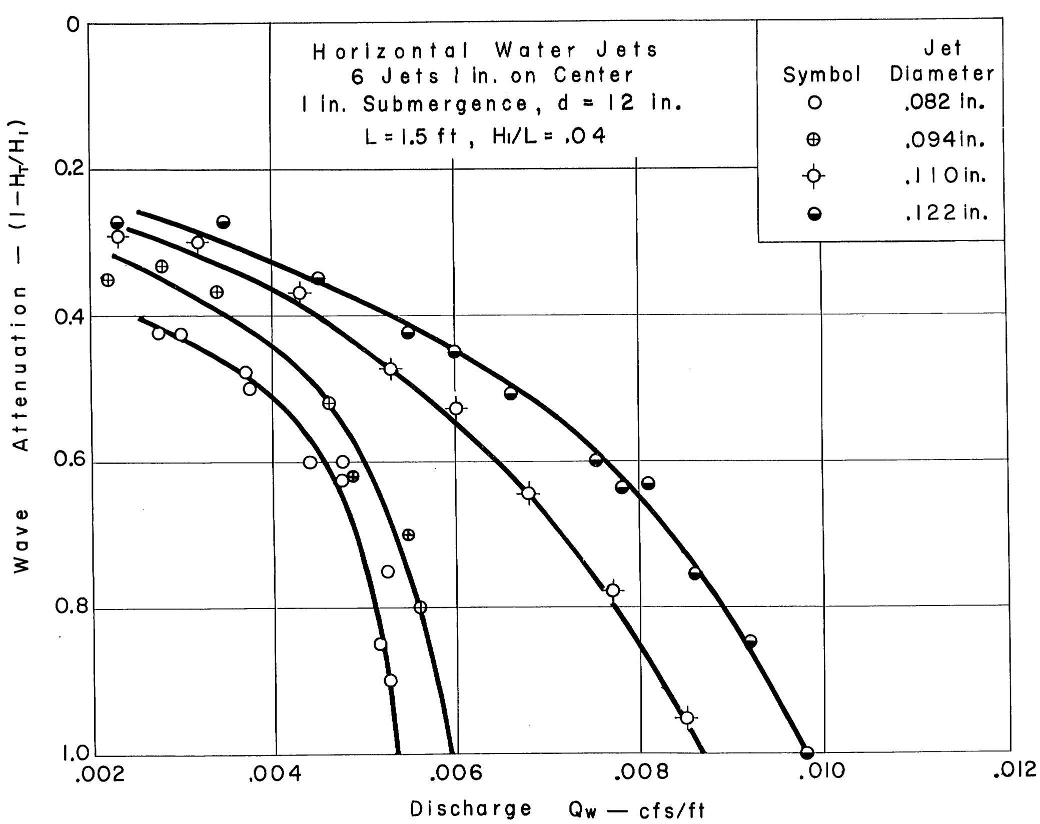

Fig. 25 - Effect of Jet Diameter on Wave Attenuation

G. Power Requirements

The small-scale studies conducted to date do not readily lend themselves to determination of prototype power requirements because of the uncertainty of the flow conditions in the manifold. However, for reference purposes some prototype horsepowers were computed at the nozzle tips with no losses considered. As a first approximation it is assumed that gravity and inertia forces are of primary importance in relating model and prototype installations, and as a consequence, that Froude's law governs. This assumption is open to question and may require modification when information is available on large-scale tests. Figure 26 is a comparison of the requirements for the 0.094-in. diameter hydraulic jets as a ratio of jet power to wave power for

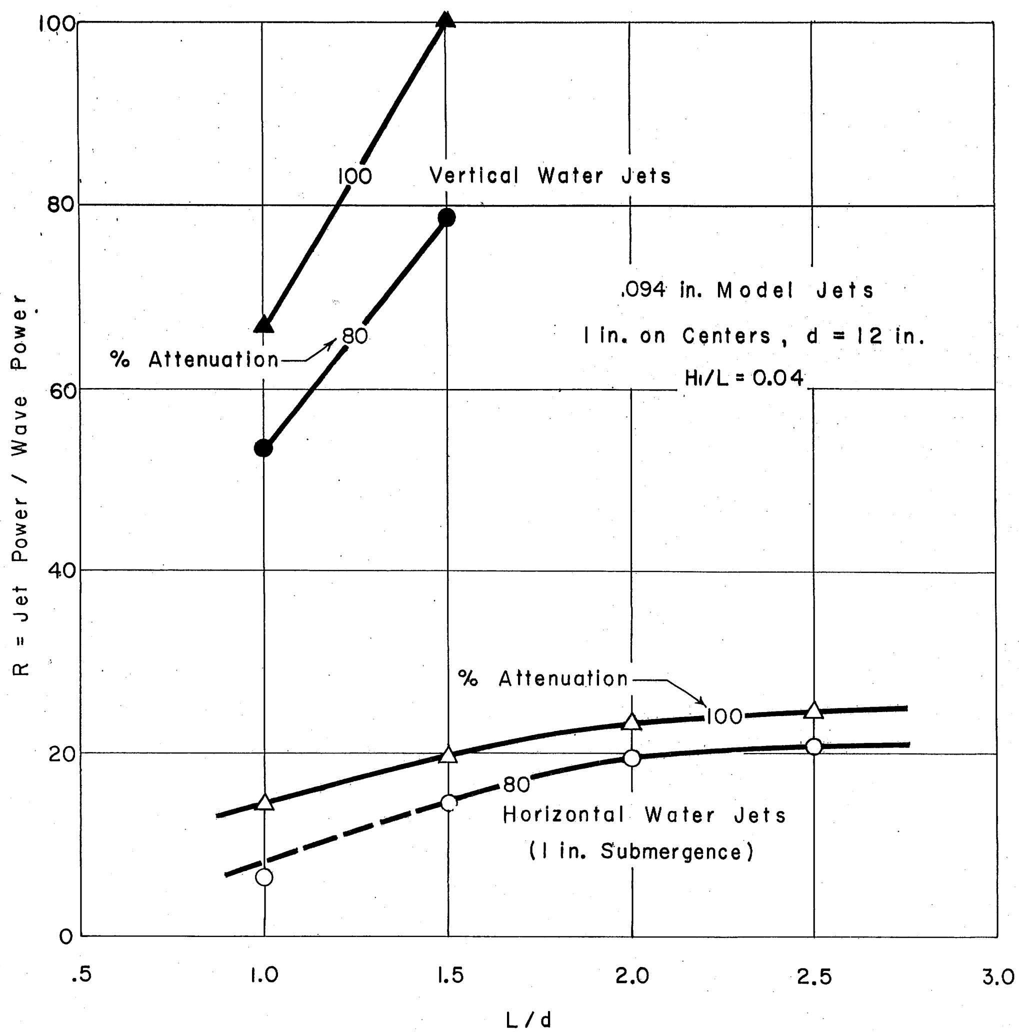

Fig. 26 - Dimensionless Plot of Hydraulic Breakwater Power Requirements

various L/d. Jet horsepower was computed by

$$HP/ft = \frac{Q_W w V_j^2}{2g(550)} \tag{15}$$

where Q_W = water discharge, cfs/ft, w = unit weight of water, lbs/ft^3, and V_j = jet velocity, fps.

The wave power was computed by the standard equation

$$HP/ft = \frac{C_g E}{L} = C_g \frac{wH^2}{8(550)} \tag{16}$$

where C_g = group velocity, fps, w = unit weight of water, lbs/ft^3, and H = wave height from trough to crest, ft.

In both cases, the horsepower was computed for a unit width. For the same attenuation and L/d, the horizontal jet is much superior to the vertical jet.

For a prototype depth of 50 ft, the vertical and horizontal water jets are compared in Fig. 27 for a model-jet diameter of 0.094 inch. The rapid increase in power requirements for waves of large L/d is readily apparent. Froude's law was used in scaling the model data to prototype conditions. It should be mentioned that the scale ratio for power varies as $L_r^{5/2}$ rather than $L_r^{7/2}$ as commonly used. The obvious reason is that the power requirements are expressed on a per ft basis, thus necessitating the dividing of the usual value of $L_r^{7/2}$ by L_r.

Considering only the horizontal water jets (since they were shown to be the most efficient), Fig. 28 shows typical horsepower requirements for various depths and values of L/d for a 90 per cent attenuation. These data are for 0.094-in. diameter model jets and 1-in. submergence. The broken lines correspond to constant wave lengths. It can be seen that the power requirements decrease for a given wave length as the water depth increases, indicating that it is most efficient to absorb waves in deep water where the ratio of wave length to water depth is small. It then appears that the primary limitations in attenuating deep-water waves are the wave length and available horsepower, the latter being of most concern.

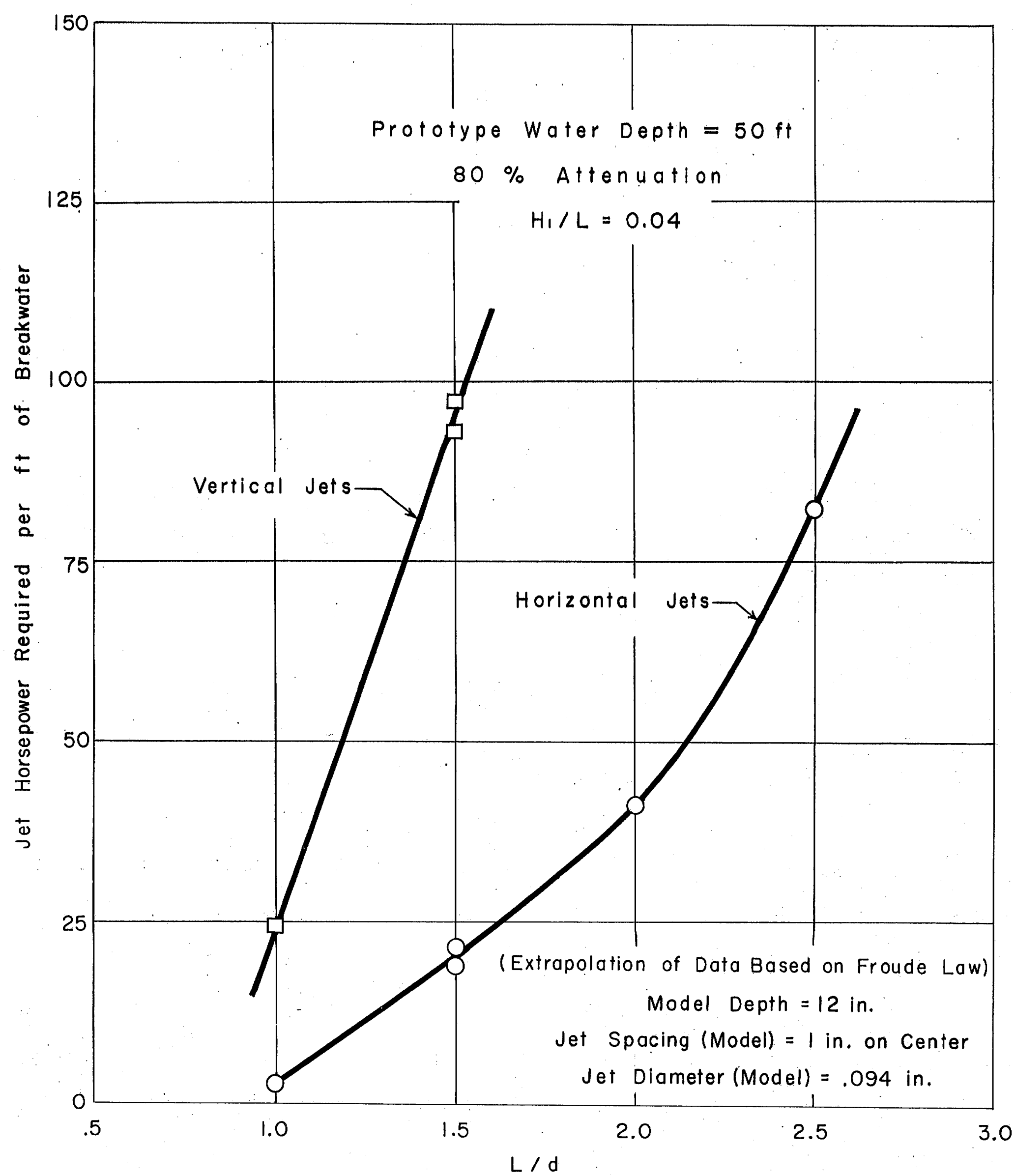

Fig. 27 – Preliminary Horsepower Requirements for Hydraulic Breakwaters

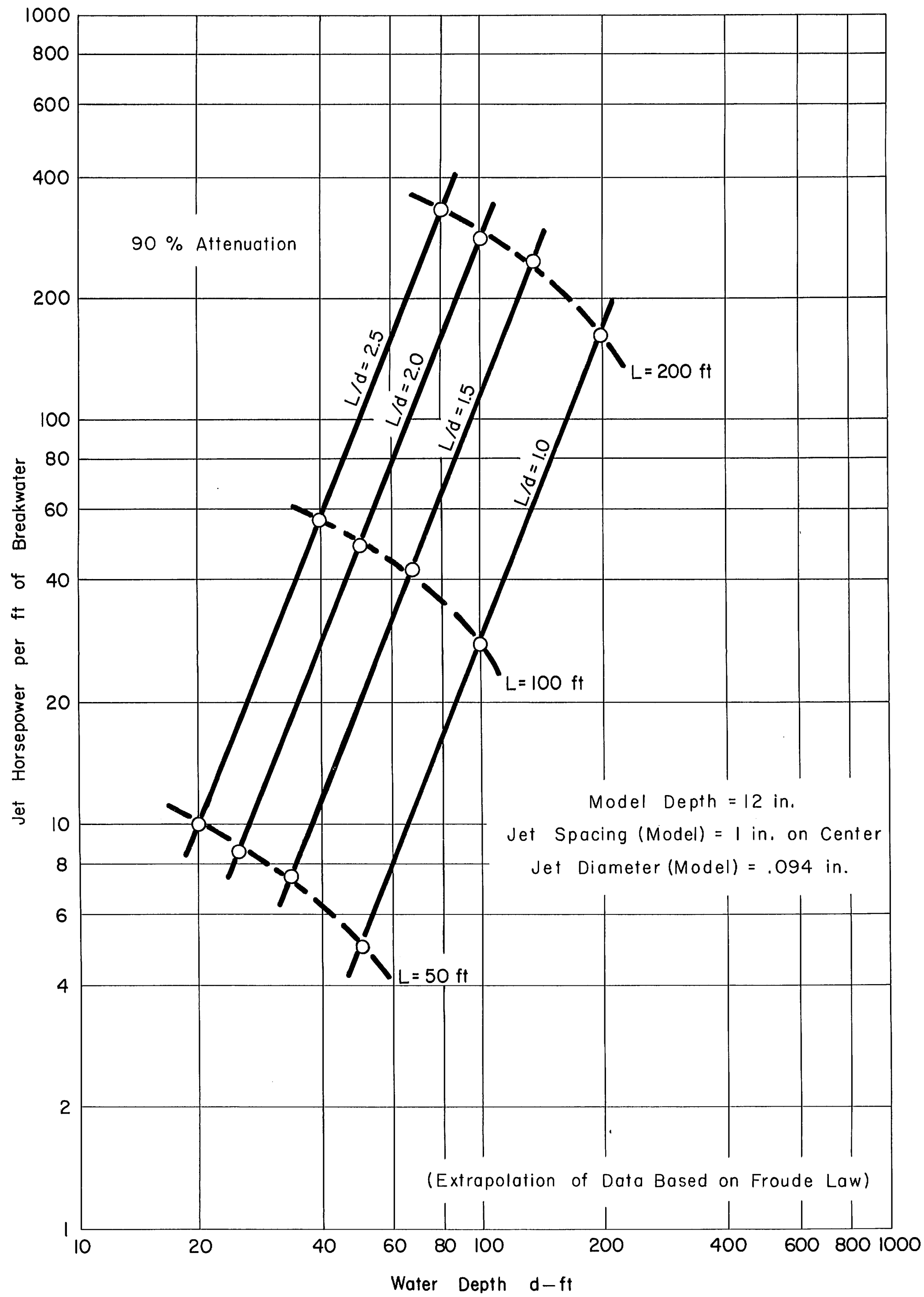

Fig. 28 - Horizontal Water-Jet Power Requirements for Various Wave Lengths and Water Depths

In making a comparison of power requirements with the pneumatic breakwater, only the horizontal water jets will be considered. A plot of this comparison is shown in Fig. 29 for a water depth of 100 ft. The pneumatic power requirements were computed by

$$HP/ft = \frac{Q_A wd}{550} \tag{17}$$

where Q_A = air discharge, cfs/ft, w = unit weight of water, lbs/ft^3, and d = water depth, ft. The perforated manifold pipe is assumed to be on the sea bed.

It appears from the preliminary data that the air jets are more effective than the water jets in attenuating the longer waves. Data computed from Taylor's theory of Section III are also plotted for comparison purposes. These computed points represent a 100 per cent attenuation. However, they still fall considerably below the values extrapolated from the model data. It is felt that the discrepancy is caused by a difference in the assumed and actual divergence of the surface current. There also may be some error caused by scale effect. More data on surface currents are necessary to verify Taylor's assumption, and it would be desirable to conduct further studies on a larger scale.

H. Pulsating Jets

A brief study was made of the effect of pulsating horizontal water jets on wave attenuation. As previously described in Section IV, the phase relationship of the jets and waves, and the duration of jet discharge could be controlled. It was found that the best results were obtained when the jet period was larger than the wave period, and the jet pulsations not necessarily being in any particular phase with the waves. Some difficulty was experienced in making accurate measurements as the pulsating jets also created waves with a period equal to the period of jet pulsation. However, several measurements were made using the 0.094-in. horizontal jets for various L/d and a 100 per cent attenuation. The jets were discharging water 50 per cent of the time and were not in phase with the incoming wave. The results of these preliminary measurements are summarized in Table III, where a comparison is made with the energy requirements of the steady horizontal water jets.

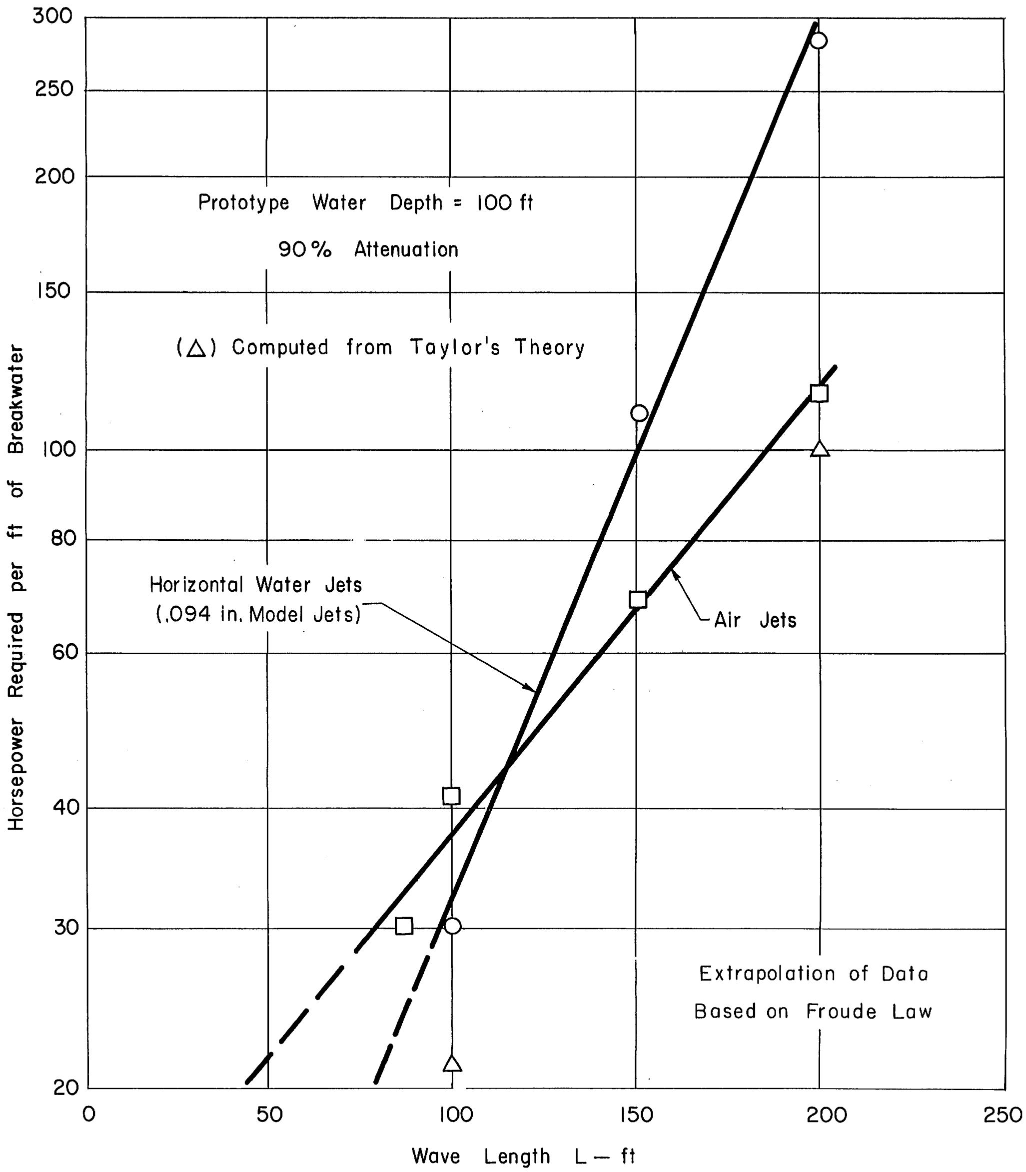

Fig. 29 – Preliminary Data on Horsepower Requirements of Pneumatic and Horizontal Water-Jet Breakwaters

TABLE III

L/d	T_p/T	Steady Q_W cfs/ft	Pulsating Q_W cfs/ft	Steady Jet Energy ft-lbs/sec	Pulsating Jet Energy ft-lbs/sec	$\frac{\text{Pulsating}}{\text{Steady}}$ Energy
1.0	1.23	0.0042	0.0038	0.217	0.321	1.48
1.5	1.44	0.0063	0.0052	0.730	0.830	1.14
2.0	3.97	0.0085	0.0064	1.800	1.465	0.82
2.5	3.54	0.0107	0.0096	3.580	5.170	1.44

The energy of the pulsating jets was computed using an average velocity head rather than an average velocity. Water hammer and other losses were not considered. From Table III it appears that the pulsating jets require slightly more energy than the steady jets. Extensive study of the pulsating jets was postponed because of time limitations and the desire to obtain data on the other parameters in the 9-ft wave tank.

VI. CONCLUSIONS

From the experimental small-scale studies on the pneumatic and hydraulic-jet breakwaters, the following conclusions may be drawn:

1. Rising air bubbles induce a vertical current which in turn creates a horizontal surface current normal to the axis of the manifold pipe. The magnitude of this current depends on the quantity of air discharged. For the tests completed, satisfactory agreement with Taylor's theory, Eq. (14), was obtained.

2. The surface currents produced by pneumatic and hydraulic breakwaters have a similar profile. However, the horizontal water jets produce a much stronger surface current and attenuate waves of larger L/d than the vertical water jets on a comparable discharge basis. The surface current moving with the direction of wave propagation has a minor effect on wave attenuation.

3. Wave attenuation by a hydraulic or water-jet breakwater is a function of wave length, water depth, jet discharge, jet submergence, jet velocity, and to a minor extent, wave steepness.

4. As the horizontal water-jet submergence is increased beyond the level at which the jets issue into the air, the discharge requirements increase for a specific deep-water wave and attenuation.

5. Both the pneumatic and the hydraulic breakwaters are effective for deep-water waves. The horizontal water jets require less horsepower than the vertical water jets for the same L/d and wave attenuation. Considering power requirements based on extrapolation of model data by Froude's law, the air jets appear to be superior to the water jets in the larger L/d region. The pulsating jets require more power than the steady horizontal water jets for the same L/d and attenuation.

B I B L I O G R A P H Y

[1] Brasher, Philip. "The Brasher Air Breakwater." The Engineer, London, Vol. 121, p. 414. May 19, 1916.

[2] Anon. Bubble Harbour. Director of Research Programmes and Planning, Admiralty Inventions Section, S.R.E., British ATR/Misc/1685, April 16, 1943. 4 pages.

[3] Schijf, J. B. "Het vernietigen van golven door het inspuiten van lucht (Pneumatische golfbrekers)." De Ingenieur, Vol. 55, pp. B.121-B.125. 1940.

[4] Carr, J. H. Mobile Breakwater Studies. California Institute of Technology, Hydrodynamics Laboratory Report No. N-642, December, 1950. 54 pages.

[5] Taylor, G. I. Note on the Possibility of Stopping Sea Waves by Means of a Curtain of Bubbles. Scientific Research Department, Admiralty, British ATR/Misc/1259, 1943. 10 pages.

[6] Biésel, F. "Étude théorique de la houle en eau courante." La Houille Blanche, pp. 278-285. May, 1950.

[7] Yi-Yuan-Yu. "Breaking of Waves by Opposing Current." American Geophysical Union Transactions, pp. 39-41. February, 1952.

APPENDIX A

APPENDIX A

Additional data from the experimental tests of the pneumatic and hydraulic breakwaters are included in this Appendix. The data are of a preliminary nature, and are included as supplementary information to the data presented in the report.

Table A-I is a tabulation of surface current data from tests of the pneumatic breakwater. The current measurements were made for various air discharges at several stations along the channel centerline and at several depths below the water surface. All measurements were made upstream of the breakwater with a small current meter. The tests were conducted with no waves present. A positive velocity indicates that the current is opposing the direction of wave propagation.

Tables A-II and A-III are tabulations of surface current data taken with the vertical and horizontal water-jet breakwater respectively. Measurements similar to those of the pneumatic breakwater were made for each of the water-jet types.

Figures A-1 and A-2 indicate the effect of vertical and horizontal water-jet discharge on wave attenuation. It is to be noted that these data were taken utilizing a different jet diameter than Figs. 19 and 20 in the report proper. It was found that the 0.094-in. jets were more efficient than the 0.082-in. jets on the basis of power requirements.

TABLE A-I

AIR JETS
SURFACE CURRENT DATA
2-4 PIPES SPACED 1-3/4 IN. ON CENTER
6-26 GAUGE NEEDLES ON EACH PIPE
d = 1 FT

Discharge cfs/ft	Distance from Jets (ft)	Depth Below Surface (ft)	Velocity fps	Discharge cfs/ft	Distance from Jets (ft)	Depth Below Surface (ft)	Velocity fps
0.0047	0.25	0.05	0.72	0.0066	1.00	0.05	0.51
		0.10	0.45			0.10	0.40
		0.15	0.23			0.15	0.31
						0.70	-0.31
0.0047	0.50	0.05	0.62			0.80	-0.28
		0.10	0.58			0.90	-0.31
		0.15	0.38				
		0.20	0.22	0.0082	0.25	0.05	0.90
		0.25	0.07			0.10	0.52
		0.60	-0.13			0.15	0.32
		0.70	-0.20			0.20	0.06
		0.80	-0.27				
		0.90	-0.30	0.0082	0.50	0.05	0.78
						0.10	0.70
0.0047	1.00	0.05	0.49			0.15	0.34
		0.10	0.34			0.20	0.16
		0.15	0.19			0.60	-0.11
		0.70	-0.14			0.70	-0.19
		0.80	-0.17			0.80	-0.24
		0.90	-0.27			0.90	-0.35
0.0066	0.25	0.05	0.72	0.0082	1.00	0.05	0.75
		0.10	0.35			0.10	0.41
		0.15	0.14			0.15	0.43
		0.60	-0.10			0.20	0.24
		0.70	-0.24			0.70	-0.18
		0.80	-0.27			0.90	-0.20
		0.90	-0.29				
				0.010	0.25	0.05	1.04
0.0066	0.50	0.05	0.70			0.10	0.59
		0.10	0.51			0.15	0.29
		0.15	0.28			0.20	0.21
		0.70	-0.15				
		0.80	-0.15				
		0.90	-0.22				

TABLE A-II

VERTICAL HYDRAULIC JETS
SURFACE CURRENT DATA
ONE ROW OF 6-0.082 IN. JETS 1 IN. ON CENTER
d = 1 FT

Discharge cfs/ft	Distance from Jets (ft)	Depth Below Surface (ft)	Velocity fps	Discharge cfs/ft	Distance from Jets (ft)	Depth Below Surface (ft)	Velocity fps
0.0048	0.25	0.05	0.50	0.0070	1.00	0.05	0.45
		0.10	0.28			0.10	0.21
		0.15	0.13			0.15	0.14
		0.20	0.04			0.20	0.10
		0.25	0.00			0.25	0.07
		0.30	0.00			0.30	0.00
		0.40	-0.03			0.40	-0.06
		0.50	-0.02			0.50	-0.03
		0.60	-0.05			0.60	-0.08
		0.70	-0.07			0.70	-0.12
		0.80	-0.10			0.80	-0.13
		0.90	-0.09			0.90	-0.18
0.0070	0.25	0.05	0.68	0.0070	1.50	0.05	0.24
		0.10	0.45			0.10	0.22
		0.15	0.13			0.15	0.07
		0.20	0.05			0.20	0.04
		0.25	0.00			0.25	0.05
		0.30	-0.02			0.30	0.04
		0.40	-0.04			0.40	0.00
		0.50	-0.06			0.50	-0.01
		0.60	-0.08			0.60	0.00
		0.70	-0.10			0.70	-0.05
		0.80	-0.13			0.80	-0.10
		0.90	-0.15			0.90	-0.08
0.0070	0.50	0.05	0.54	0.0070	2.00	0.05	0.10
		0.10	0.32			0.10	0.05
		0.15	0.21			0.15	0.09
		0.20	0.08			0.20	0.03
		0.25	0.00			0.25	0.03
		0.30	-0.04			0.30	0.04
		0.40	-0.07			0.40	0.00
		0.50	-0.07			0.50	0.00
		0.60	-0.06			0.60	0.00
		0.70	-0.12			0.70	0.00
		0.80	-0.12			0.80	-0.02
		0.90	-0.12			0.90	-0.08

TABLE A-II (Cont.)

VERTICAL HYDRAULIC JETS
SURFACE CURRENT DATA
ONE ROW OF 6-0.082 IN. JETS 1 IN. ON CENTER
d = 1 FT

Discharge cfs/ft	Distance from Jets (ft)	Depth Below Surface (ft)	Velocity fps	Discharge cfs/ft	Distance from Jets (ft)	Depth Below Surface (ft)	Velocity fps
0.0082	0.25	0.05	0.78	0.0082	2.00	0.05	0.23
		0.10	0.40			0.10	0.19
		0.15	0.18			0.15	0.14
		0.20	0.03			0.20	0.14
		0.25	0.00			0.25	0.11
		0.30	-0.06			0.30	0.07
		0.40	-0.07			0.40	0.02
		0.50	-0.07			0.50	-0.05
		0.60	-0.13			0.60	-0.06
		0.70	-0.15			0.70	-0.11
		0.80	-0.16			0.80	-0.20
		0.90	-0.18			0.90	-0.25
0.0082	1.00	0.05	0.65	0.0092	0.25	0.05	0.87
		0.10	0.29			0.10	0.44
		0.15	0.24			0.15	0.09
		0.20	0.20			0.20	0.00
		0.25	0.00			0.25	0.00
		0.30	0.00				
		0.40	-0.03	0.0092	0.50	0.05	0.71
		0.50	-0.09			0.10	0.42
		0.60	-0.17			0.15	0.19
		0.70	-0.16			0.20	0.06
		0.80	-0.27			0.25	0.03
		0.90	-0.27			0.30	0.00
0.0082	1.50	0.05	0.42	0.0092	1.00	0.05	0.52
		0.10	0.35			0.10	0.24
		0.15	0.15			0.15	0.17
		0.20	0.22			0.20	0.14
		0.25	0.13			0.25	0.06
		0.30	0.03			0.30	0.00
		0.40	-0.02				
		0.50	-0.08	0.0092	1.50	0.05	0.25
		0.60	-0.13			0.10	0.23
		0.70	-0.21			0.15	0.12
		0.80	-0.23			0.20	0.03
		0.90	-0.35			0.25	0.06
						0.30	0.04
						0.40	0.00

TABLE A-III

HORIZONTAL HYDRAULIC JETS
SURFACE CURRENT DATA
ONE ROW OF 6-0.082 IN. JETS 1 IN. ON CENTER
d = 1 FT

Discharge cfs/ft	Distance from Jets (ft)	Depth Below Surface (ft)	Velocity fps
0.0040	0.50	0.05	0.63
		0.10	0.55
		0.15	0.42
		0.20	0.00
0.0040	1.00	0.05	0.55
		0.10	0.49
		0.15	0.30
		0.20	0.10
		0.25	0.00
0.0040	2.00	0.05	0.33
		0.10	0.25
		0.15	0.20
		0.20	0.18
		0.25	0.10
		0.30	0.05
		0.40	0.00
0.0040	3.00	0.05	0.41
		0.10	0.34
		0.15	0.29
		0.20	0.19
		0.25	0.13
		0.30	0.08
		0.40	0.00
		0.50	0.00
		0.60	-0.09
		0.70	-0.16
		0.80	-0.19
		0.90	-0.25
0.0060	1.00	0.05	0.87
		0.10	0.72
		0.15	0.48
		0.20	0.27
		0.25	0.07
		0.30	0.00
		0.40	-0.10
		0.50	-0.16
		0.60	-0.18
		0.70	-0.21
		0.80	-0.18
		0.90	-0.20
0.0060	1.50	0.05	0.70
		0.10	0.56
		0.15	0.46
		0.20	0.31
		0.25	0.13
		0.30	0.05
		0.40	-0.05
		0.50	-0.11
		0.60	-0.21
		0.70	-0.19
		0.80	-0.23
		0.90	-0.25
0.0060	3.00	0.05	0.50
		0.10	0.38
		0.15	0.38
		0.20	0.28
		0.25	0.21
		0.30	0.15
		0.40	0.03
		0.50	-0.04
		0.60	-0.09
		0.70	-0.20
		0.80	-0.21
		0.90	-0.27
0.0075	0.50	0.05	1.50
		0.10	0.93
		0.15	0.19
		0.20	0.00
0.0075	1.00	0.05	1.21
		0.10	0.91
		0.15	0.44
		0.20	0.16
		0.25	0.00
0.0075	2.00	0.05	0.96
		0.10	0.69
		0.15	0.46
		0.20	0.27
		0.25	0.11
		0.30	0.00

TABLE A-III (Cont.)

HORIZONTAL HYDRAULIC JETS
SURFACE CURRENT DATA
ONE ROW OF 6-0.082 IN. JETS 1 IN. ON CENTER
d = 1 FT

Discharge cfs/ft	Distance from Jets (ft)	Depth Below Surface (ft)	Velocity fps	Discharge cfs/ft	Distance from Jets (ft)	Depth Below Surface (ft)	Velocity fps
0.0075	3.00	0.05	0.52	0.0100	2.50	0.05	0.84
		0.10	0.53			0.10	0.79
		0.15	0.32			0.15	0.53
		0.20	0.27			0.20	0.34
		0.25	0.16			0.25	0.24
		0.30	0.07			0.30	0.13
		0.40	0.00			0.40	0.00
0.0100	0.50	0.05	1.86	0.0100	3.00	0.05	0.95
		0.10	1.70			0.10	0.81
		0.15	0.77			0.15	0.59
		0.20	0.24			0.20	0.48
		0.25	-0.15			0.25	0.34
						0.30	0.25
0.0100	1.00	0.05	1.50			0.40	0.10
		0.10	1.21			0.50	-0.08
		0.15	0.70			0.60	-0.26
		0.20	0.51			0.70	-0.38
		0.25	0.12			0.80	-0.48
		0.30	0.00			0.90	-0.53
		0.40	-0.11				
		0.50	-0.22	0.0100	3.50	0.05	0.58
		0.60	-0.16			0.10	0.50
		0.70	-0.25			0.15	0.41
		0.80	-0.24			0.20	0.38
		0.90	-0.26			0.25	0.25
						0.30	0.19
0.0100	1.50	0.10	1.04			0.40	0.13
		0.20	0.53			0.50	0.00
		0.30	0.06				
		0.40	-0.11	0.0100	4.00	0.05	0.33
		0.50	-0.30			0.10	0.38
		0.60	-0.35			0.15	0.44
		0.70	-0.48			0.20	0.26
		0.80	-0.51			0.25	0.27
		0.90	-0.54			0.30	0.21
						0.40	0.12
0.0100	2.50	0.05	1.12			0.50	0.06
		0.10	0.89			0.60	-0.00
		0.20	0.51				
		0.30	0.24				
		0.40	-0.06				
		0.50	-0.22				
		0.60	-0.34				
		0.70	-0.54				
		0.80	-0.62				
		0.90	-0.69				

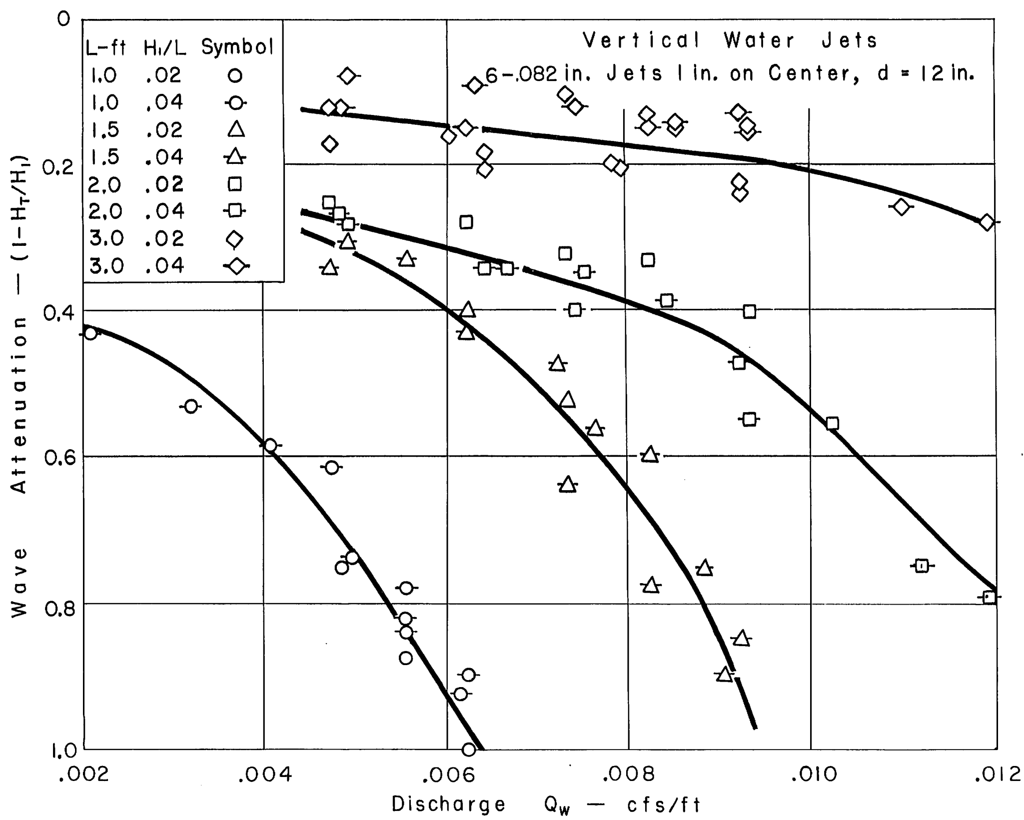

Fig. A-1 - Effect of Vertical Water-Jet Discharge on Wave Attenuation (0.082 in. Diameter Jets)

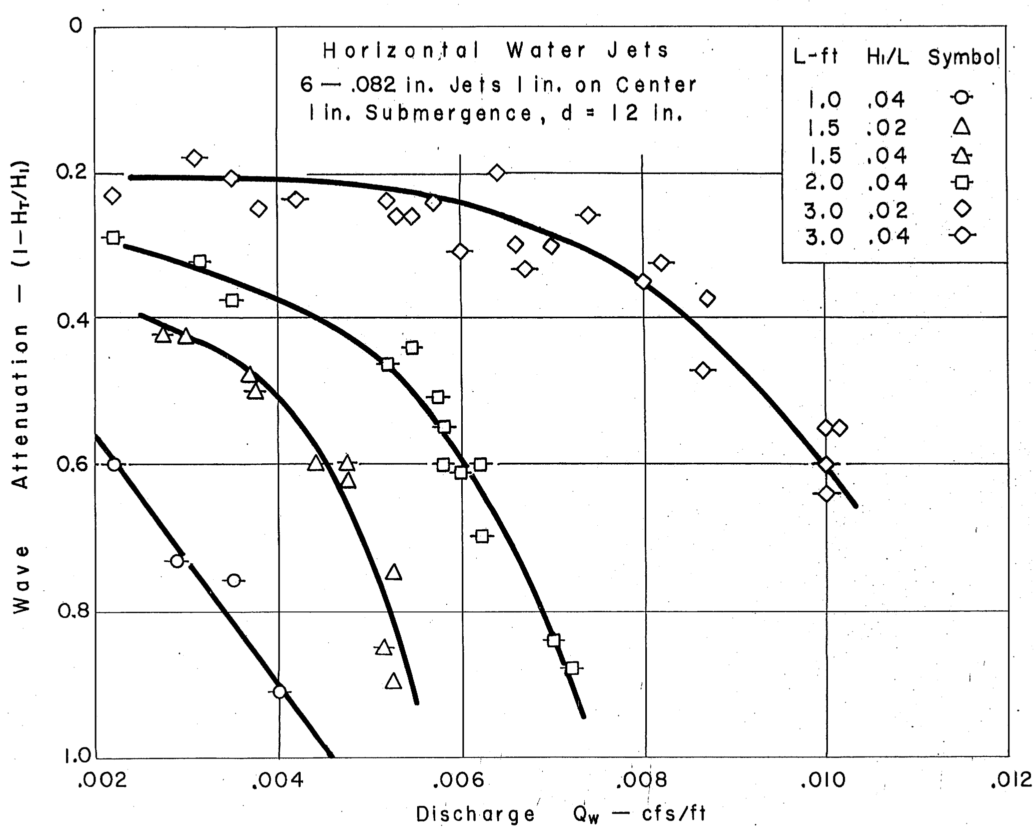

Fig. A-2 - Effect of Horizontal Water-Jet Discharge on Wave Attenuation (0.082 in. Diameter Jets)

DISTRIBUTION LIST FOR PROJECT REPORT NO. 46

of the St. Anthony Falls Hydraulic Laboratory

Copies	Organization
2	Chief of Naval Research, Department of the Navy, Washington 25, D. C., Attn: Code 438.
1	Commanding Officer, Office of Naval Research, Branch Office, The John Crerar Library Bldg., 86 East Randolph Street, Chicago 1, Illinois.
1	Commanding Officer, Office of Naval Research, Branch Office, 346 Broadway, New York 13, New York.
1	Commanding Officer, Office of Naval Research, Branch Office, 1030 East Green Street, Pasadena 1, California.
1	Commanding Officer, Office of Naval Research, Branch Office, 1000 Geary Street, San Francisco 24, California.
2	Commanding Officer, Office of Naval Research, Navy #100, Fleet Post Office, New York, New York.
6	Director, Naval Research Laboratory, Washington 25, D. C., Attn: Code 2021.
5	Documents Service Center, Armed Services Technical Information Agency, Knott Building, Dayton 2, Ohio.
1	Chief, Bureau of Aeronautics, Department of the Navy, Washington 25, D. C., Attn: Research Division.
1	Chief, Bureau of Ordnance, Department of the Navy, Washington 25, D. C., Attn: Research and Development Division.
1	Office of Ordnance Research, Department of the Army, Washington 25, D. C.
1	Commander, Air Research and Development Command, P. O. Box 1395, Baltimore 18, Maryland, Attn: Fluid Mechanics Division.
1	Director of Research, National Advisory Committee for Aeronautics, 1512 H Street, N. W., Washington 25, D. C.
1	Director, Langley Aeronautical Laboratory, National Advisory Committee for Aeronautics, Langley Field, Virginia.
1	Director, National Bureau of Standards, Washington 25, D. C., Attn: Fluid Mechanics Section.
1	Professor R. Courant, Institute for Mathematics and Mechanics, New York University, 45 Fourth Avenue, New York 3, New York.

Copies	Organization
1	Professor G. Kuerti, Department of Mechanical Engineering, Case Institute of Technology, Cleveland, Ohio.
1	Professor W. R. Sears, Director, Graduate School of Aeronautical Engineering, Cornell University, Ithaca, New York.
1	Chief, Bureau of Yards and Docks, Department of the Navy, Washington 25, D. C., Attn: Research Division.
1	Commanding Officer and Director, David Taylor Model Basin, Washington 7, D. C., Attn: Ship Division.
1	Hydrographer, Department of the Navy, Washington 25, D. C.
1	Director, Waterways Experiment Station, Box 631, Vicksburg, Mississippi.
1	Office of the Chief of Engineers, Department of the Army, Gravelly Point, Washington 25, D. C.
1	Beach Erosion Board, U. S. Army Corps of Engineers, Washington 25, D. C.
1	Commissioner, Bureau of Reclamation, Washington 25, D. C.
1	Dr. G. H. Keulegan, National Hydraulic Laboratory, National Bureau of Standards, Washington 25, D. C.
1	Brown University, Division of Applied Mathematics, Providence 12, Rhode Island.
2	California Institute of Technology, Hydrodynamics Laboratory, Pasadena 4, California, Attn: [Professor M. S. Plesset (1), Professor V. A. Vanoni (1)].
1	Professor M. L. Albertson, Department of Civil Engineering, Colorado A & M College, Fort Collins, Colorado.
1	Professor G. Birkhoff, Department of Mathematics, Harvard University, Cambridge 38, Massachusetts.
1	Massachusetts Institute of Technology, Department of Naval Architecture, Cambridge 39, Massachusetts.
1	Dr. R. R. Revelle, Scripps Institute of Oceanography, La Jolla, California.
1	Stanford University, Applied Mathematics and Statistics Laboratory, Stanford, California.
1	Professor J. W. Johnson, Fluid Mechanics Laboratory, University of California, Berkeley 4, California.

Copies	Organization
1	Professor H. A. Einstein, Department of Engineering, University of California, Berkeley 4, California.
1	Dean K. E. Schoenherr, College of Engineering, University of Notre Dame, Notre Dame, Indiana.
1	Director, Woods Hole Oceanographic Institute, Woods Hole, Massachusetts.
2	Chief, Bureau of Ships, Department of the Navy, Washington 25, D. C., Attn: [Research Division (1), Code 420 (Preliminary Design Division) (1)].
1	Commander, Naval Ordnance Test Station, 3202 E. Foothill Blvd., Pasadena, California.
3	Commanding Officer and Director, David Taylor Model Basin, Washington 7, D. C., Attn: [Hydromechanics Lab. (1), Hydrodynamics Div. (1), Library (1)].
1	California Institute of Technology, Hydrodynamics Laboratory, Pasadena 4, California.
1	Professor A. T. Ippen, Hydrodynamics Laboratory, Massachusetts Institute of Technology, Cambridge 38, Massachusetts.
1	Dr. Hunter Rouse, Director, Iowa Institute of Hydraulic Research, State University of Iowa, Iowa City, Iowa.
1	Stevens Institute of Technology, Experimental Towing Tank, 711 Hudson Street, Hoboken, New Jersey.
1	Dr. L. G. Straub, St. Anthony Falls Hydraulic Laboratory, University of Minnesota, Minneapolis 14, Minnesota.
1	Mr. George Hickox, Program Director for Engineering Sciences, National Science Foundation, Washington 25, D. C.
1	Mr. C. A. Gongwer, Aerojet General Corporation, 6352 N. Irwindale Avenue, Azusa, California.
1	Hydraulics Laboratory, Michigan State College, East Lansing, Michigan, Attn: Professor H. R. Henry.